

Copper availability governs nitrous oxide accumulation in wetland soils and stream sediments

Neha Sharma,¹ Elaine D. Flynn,² Jeffrey G. Catalano² and Daniel E. Giammar^{1*}

¹*Department of Energy, Environmental and Chemical Engineering, Washington University in St. Louis, St. Louis, Missouri 63130, United States*

²*Department of Earth and Planetary Sciences, Washington University in St. Louis, St. Louis, Missouri 63130, United States*

*Corresponding Author:

Address: Department of Energy, Environmental and Chemical Engineering, Washington University in St. Louis, St. Louis, MO 63130, USA

Phone: (314) 935-6849

Email: giammar@wustl.edu

Revised manuscript submitted to *Geochimica et Cosmochimica Acta*

January 2022

This paper is a non-peer reviewed preprint submitted to EarthArXiv

1 **ABSTRACT**

2 Denitrification is microbially-mediated through enzymes containing metal cofactors. Laboratory studies of
3 pure cultures have highlighted that the availability of Cu, required for the multicopper enzyme nitrous oxide
4 reductase, can limit N₂O reduction. However, in natural aquatic systems, such as wetlands and hyporheic
5 zones in stream beds, the role of Cu in controlling denitrification remains incompletely understood. In this
6 study, we collected soils and sediments from three natural environments -- riparian wetlands, marsh
7 wetlands, and a stream -- to investigate their nitrogen species transformation activity at background Cu
8 levels and different supplemented Cu loadings. All of the systems contained solid-phase associated Cu
9 below or around geological levels (40 - 280 nmol g⁻¹) and exhibited low dissolved Cu (3-50 nM), which
10 made them appropriate sites for evaluating the effect of limited Cu availability on denitrification. In
11 laboratory incubation experiments, high concentrations of N₂O accumulated in all microcosms lacking Cu
12 amendment except for one stream sediment sample. With Cu added to provide dissolved concentrations at
13 trace levels (10-300 nM), reduction rate of N₂O to N₂ in the wetland soils and stream sediments was
14 enhanced. A kinetic model could account for the trends in nitrogen species by combining the reactions for
15 microbial reduction of NO₃⁻ to NO₂⁻/N₂O/N₂ and abiotic reduction of NO₂⁻ to N₂. The model revealed that
16 the rate of N₂O to N₂ conversion increased significantly in the presence of Cu. For riparian wetland soils
17 and stream sediments, the kinetic model also suggested that overall denitrification is driven by abiotic
18 reduction of NO₂⁻ in the presence of inorganic electron donors. This study demonstrated that natural aquatic
19 systems containing Cu at concentrations less than or equal to crustal abundances may display incomplete
20 reduction of N₂O to N₂ that would cause N₂O accumulation and release to the atmosphere.

21 **Keywords:** wetlands, hyporheic zone, denitrification, nitrous oxide, copper, bioavailability, organic carbon

22 **1. Introduction**

23 Nitrous oxide (N_2O) is a potent greenhouse gas whose global warming potential per unit mass is 265–298
24 times that of carbon dioxide (CO_2) for a 100-year timescale (IPCC, 2014; Sovacool et al., 2021). Global
25 N_2O emissions in the decade between 2007–2016 averaged 17 Tg N yr^{-1} , of which 57% (9.7 Tg N yr^{-1}) were
26 from natural soils and oceans and ~22% (3.8 Tg N yr^{-1}) were from agricultural soils (Tian et al., 2020).
27 Denitrification, an anoxic process in which nitrate (NO_3^-) is reduced to N_2 , is a key biogeochemical process
28 that regulates the amount of N_2O released from both terrestrial and aquatic ecosystems into the atmosphere
29 (Makowski, 2019; Tian et al., 2020; Martinez-Espinosa et al., 2021). Natural aquatic systems, especially
30 those that display vertical redox gradients, such as wetlands and hyporheic zones in streams, are active sites
31 for denitrification (Merill and Tonjes, 2014; Nag et al., 2017; Mwagona et al., 2019; Martinez-Espinosa et
32 al., 2021). Oxic regions above redox transition zones favor the oxidation of ammonia (NH_3) to NO_3^- via
33 nitrification, and the anoxic regions below redox transition zones promote denitrification with NO_3^- being
34 reduced to nitrite (NO_2^-), nitric oxide (NO), N_2O , and N_2 . The incomplete conversion of NO_3^- and NO_2^- to
35 N_2 causes N_2O to be released from the aquatic systems to the atmosphere (Twining et al., 2007;
36 Giannopoulos et al., 2020).

37 An array of metalloenzymes that contain Fe, Cu, and Mo are involved in reducing nitrate and
38 intermediate species to N_2 during denitrification (Godden et al., 1991; Bertero et al., 2003; Nojiri et al.,
39 2007). The transformation of NO_3^- to NO_2^- is catalyzed by respiratory nitrate reductase (Nar), which requires
40 Fe and Mo for complete conversion (Bertero et al., 2003; Jormakka et al., 2004). Depending on the type of
41 microorganism, reduction of NO_2^- to NO is catalyzed by either an iron-containing nitrite reductase (NirS)
42 or a Cu-containing nitrite reductase (NirK) (Godden et al., 1991; Nojiri et al., 2007). NO is rapidly
43 transformed to N_2O with an Fe-bearing nitric oxide reductase (cNOR), and in the final step, N_2O is reduced
44 to N_2 by a Cu-rich nitrous oxide reductase (Nos) (Brown et al., 2000).

45 A scarcity of available Cu can limit the conversion of N_2O to N_2 . Laboratory studies of pure cultures
46 have demonstrated that Cu limitation resulted in N_2O accumulation (Iwasaki et al., 1980; Granger and Ward,

47 2003; Black et al., 2016). Granger and Ward (2003) conducted a study with *Pseudomonas stutzeri* and
48 *Paracoccus denitrificans* in an artificial seawater medium to evaluate the effect of Cu on denitrification.
49 They observed that Cu concentrations of approximately 3 nM caused N₂O to accumulate, whereas 10 nM
50 Cu resulted in increased growth rates and complete conversion of N₂O to N₂. The growth of denitrifying
51 microorganisms, *Alcaligenes* sp. NGIB 11015, *Alcaligenes faecalis* IAM 1015, and *P. stutzeri* was also
52 stimulated by the addition of Cu in the range of 0.5 to 80 μM (Iwasaki et al., 1980; Black et al., 2016).

53 In soils and sediments, high concentrations of Cu can inhibit denitrification, whereas low
54 availability of Cu can limit microbial activity causing accumulation of intermediate nitrogen species. In
55 estuarine sediments, the addition of 79 μg g⁻¹ Cu inhibited microbial activity by 85% and specifically
56 increased the accumulation of NO₂⁻ and N₂O (Magalhaes et al., 2007). Similarly, the addition of Cu at high
57 loadings of 250-1000 μg g⁻¹ increased N₂O emissions from soils and wetland sediments (Sakadevan et al.,
58 1999; Shaaban et al., 2019). In these three studies, the associated dissolved Cu concentrations were not
59 measured. While the three studies just noted had increased accumulation of N₂O associated with high Cu,
60 two other studies found that the addition of Cu to systems with initially low Cu decreased N₂O accumulation.
61 A recent study of freshwater wetland sediments that initially had 37.8 μg g⁻¹ Cu and were amended with
62 CuSO₄ to have 26 μM dissolved Cu showed an increased abundance of nitrite and nitrous oxide reductase
63 genes that enhanced the conversion of N₂O to N₂ (Giannopoulos et al., 2020). Similarly, a study of
64 freshwater sediments collected from central Indiana also showed that N₂O accumulation decreased when
65 the sediments were amended with 50-100 μg g⁻¹ Cu (Jacinthe and Tedesco, 2009). On the other hand, the
66 addition of 100 μg L⁻¹ Cu did not have any effect on N₂O emissions release in freshwater wetland sediments
67 (Doroski et al., 2019). Copper concentrations in uncontaminated environments are typically low (Black et
68 al., 2011; Black et al., 2016), and hence limited Cu bioavailability in such settings may significantly affect
69 N₂O conversion via denitrification.

70 In natural aquatic systems, the relationship between the total Cu amount in the sediments and the
71 bioavailable concentration of dissolved Cu is controlled by the presence of solid phases, such as sulfide
72 minerals, particulate organic carbon, iron and manganese oxyhydroxides, and clay minerals (Du Laing et

73 al., 2009; Campana et al., 2012; Bourgeault et al., 2013; Zhang et al., 2014). Changes in aquatic phase
74 parameters, including pH, redox potential, and the concentration of ligands, can mobilize/immobilize
75 metals from solid phases, thus affecting their bioavailability (Du Laing et al., 2009; Zhang et al., 2014).
76 Dissolved Cu is present as a free hydrated ion (Cu^{2+}) and complexes with hydroxides, inorganic ligands
77 (carbonates and chlorides), and organic ligands (humic and fulvic acids) depending on the water
78 composition (Kozelka and Bruland, 1998). Strong organic Cu-chelates, such as complexes with humic acids
79 and fulvic acids, are inert and hence not readily bioavailable, but inorganic hydroxy and carbonate
80 complexes are labile and might be toxic to some microorganisms at concentrations as low as $10 \mu\text{g L}^{-1}$
81 (Allen and Hansen, 1996; Bruland et al., 2000; Huang and Wang, 2003; Bourgeault et al., 2013). Several
82 studies have reported that Cu has a high affinity for dissolved organic carbon and exists predominantly as
83 Cu-organic ligand complexes in natural waters (Skrabal et al., 2000; Chakraborty et al., 2015; Ren et al.,
84 2015; Waska et al., 2019). Thus, even dissolved Cu concentrations that would be expected to be optimal
85 for N_2O conversion ($>10 \text{ nM}$) might exert a limiting effect on denitrification in natural environments if the
86 Cu is predominantly complexed in non-bioavailable forms.

87 In natural environments, nitrogen cycling can also occur via processes other than biological
88 denitrification. These processes include dissimilatory nitrate reduction to ammonium (DNRA), anaerobic
89 ammonium oxidation (anammox), chemoautotrophic denitrification, and abiotic photochemical and
90 thermochemical processes (Burgin and Hamilton, 2007; Doane, 2017; Martinez-Espinosa et al., 2021).
91 Other elemental cycles, such as those of iron and sulfur, play important roles in nitrogen cycling in natural
92 environments. Autotrophic and mixotrophic denitrifiers can gain energy from mediating the reduction of
93 NO_3^- by inorganic electron donors that include sulfur compounds (S^0 , S^{2-} , $\text{S}_2\text{O}_3^{2-}$), pyrite (FeS_2), Fe^{2+} , Fe^0 ,
94 and Mn^{2+} (Davidson et al., 2003; Weber et al., 2006; Melton et al., 2014; Di Capua et al., 2019; Wei et al.,
95 2019). Additionally, abiotic reduction of $\text{NO}_3^-/\text{NO}_2^-$ by dissolved Fe(II) or Fe(II)-bearing minerals has been
96 studied extensively as a pathway for N_2O or N_2 formation under anoxic conditions (Moraghan and Buresh,
97 1977; Ottley et al., 1997; Matocha et al., 2012; Melton et al., 2014; Peters et al., 2014; Buchwald et al.,
98 2016; Liu et al., 2019; Matus et al., 2019; Chen et al., 2020). Fe(II)-rich flooded soils showed decreased

99 N₂O emissions because high Fe(II) concentrations favored the complete conversion of NO₃⁻ to N₂ (Wang et
100 al., 2016). A recent study of marine sediments found that ~15-25% of the total N₂O released was produced
101 by abiotic nitrite reduction in the presence of Fe(II) (Otte et al., 2019).

102 The effects of redox conditions, substrate availability, temperature, and pH on denitrification have
103 been widely studied (Nowicki, 1994; Koponen et al., 2004; Baeseman et al., 2006; Ward et al., 2008; Nag
104 et al., 2017). There has also been significant progress in understanding the toxic effects of elevated Cu
105 levels on the denitrification pathway, but only limited studies have investigated the effect of Cu availability
106 on N₂O accumulation in uncontaminated aquatic systems (Twining et al., 2007; Giannopoulos et al., 2020).
107 A broader understanding of how Cu affects N-cycling in natural systems can improve the accuracy of
108 ecosystem models, such as the Dynamic Land Ecosystem Model (DLEM) (Tian et al., 2020), used to
109 estimate N₂O emissions. The objectives of this study were to (1) investigate the effect of trace
110 concentrations of dissolved Cu on nitrate reduction and the formation of reaction products (NO₂⁻ and N₂O)
111 with soils and sediments from three different natural aquatic systems and (2) develop a kinetic model for
112 the denitrification reactions that can quantify the effect of Cu addition on the transformation and
113 accumulation of nitrogen species in environmental systems.

114 **2. Materials and methods**

115 **2.1 Description of sites**

116 To investigate the effect of Cu on denitrification, we selected three separate natural aquatic systems: marsh
117 wetlands at Argonne National Laboratory (ANL) in Lemont, Illinois; riparian wetlands in the Tims Branch
118 (TB) watershed at the Savannah River Site in Aiken County, South Carolina; and East Fork Poplar Creek
119 (EFPC) at Oak Ridge National Laboratory (ORNL) in Oak Ridge, Tennessee. Detailed information on the
120 sampling sites, sampling techniques, and soil characterization can be found in our recent study on trace
121 metal speciation at these sites (Yan et al., 2021). Briefly, soil/sediment and surface water samples were
122 collected from two different locations at each aquatic system. To identify locations within the sites, we used

123 the labels “Riparian 1” and “Riparian 2” for Tims Branch riparian wetland soils; “Stream 1” and “Stream
124 2” for Oak Ridge stream sediment sites, and “Marsh 1” and “Marsh 2” for Argonne marsh wetland soils.

125 **2.2 Sampling and characterization**

126 Soil or sediment cores were collected in polycarbonate tubes. Cores from the marsh wetland and
127 riparian wetland were shipped on ice to Washington University in St. Louis, where they were extruded from
128 the tubes and immediately transferred to an anaerobic chamber (Coy Laboratory Products, 3% H₂/97% N₂,
129 with Pd catalyst) to maintain anaerobic conditions. The cores from the stream sediment site were extruded
130 at ORNL within 1 h of sampling, impulse sealed in polyethylene pouches in an anaerobic chamber, and
131 stored in a refrigerator at 4°C before being shipped on ice to Washington University, where they were stored
132 in an anaerobic chamber.

133 Surface water samples were filtered using 0.22 µm mixed cellulose ester (MCE) syringe filters. A
134 portion was immediately acidified to 2% nitric acid (HNO₃), and the rest of the filtered water was stored at
135 4 °C prior to anion and nutrient analysis. The acidified surface water samples were analyzed to quantify the
136 dissolved major elements (sodium, magnesium, aluminum, silicon, potassium, and calcium) and trace
137 metals (cobalt, nickel, copper, and zinc). The major elements were quantified using a Thermo Scientific
138 iCap 7400 Duo inductively-coupled plasma optical emission spectrometer (ICP-OES), and the trace metals
139 were quantified with an inductively coupled plasma mass spectrometer (PerkinElmer Elan DRC II). The
140 unacidified water samples were used to measure the concentrations of dissolved anions (Br⁻, Cl⁻, F⁻, and
141 SO₄²⁻) using a Thermo Scientific Dionex Integrion high-pressure ion chromatograph (IC) with a
142 conductivity detector. The major elements and trace metals were extracted from the soils/sediments by
143 microwave-assisted digestion and were analyzed using ICP-OES and ICP-MS, respectively (Yan et al.,
144 2021). The extractable nutrients (nitrate, ammonium, and phosphate) in the soils and sediments were
145 obtained using a 2 M potassium chloride extraction method adapted from previous studies (Sparks et al.,
146 1996; Pansu and Gautheyrou, 2006) and were measured using a Seal Analytical AQ300 Discrete Multi-
147 Chemistry Analyzer.

148 **2.3 Reagent preparation**

149 All the solutions were prepared in an anaerobic chamber (3% H₂/97% N₂, with Pd catalyst) using
150 deoxygenated deionized water (>18.2 MΩ cm). Deoxygenated water was prepared by bubbling N₂ gas
151 through it for 4-5 h, followed by bubbling the water in an anaerobic chamber for 3 h with a filtered stream
152 of the anaerobic chamber atmosphere that had been passed in sequence through solutions of ferrous chloride
153 and KOH to remove traces of oxygen and carbon dioxide. A colorimetric assay (CHEMets test kit K-7511)
154 was used to ensure that the dissolved oxygen level in the deoxygenated water was below the detection limit
155 (2 µg/L). Copper chloride dihydrate (99.99%, Sigma Aldrich) was used to vary the Cu loading in
156 denitrification studies. All other salts (sodium chloride, potassium chloride, sodium sulfate, magnesium
157 chloride hexahydrate, magnesium sulfate, calcium sulfate dihydrate, ammonium chloride, and disodium
158 phosphate) used for preparing simulated site water were purchased from Thermo Fisher Scientific and were
159 of reagent grade. Sodium nitrate and potassium nitrate (99.9%, Sigma Aldrich) were used for preparing a
160 stock solution of nitrate. Nitric acid (trace metal grade, Thermo Fisher Scientific) was used to acidify
161 samples for dissolved metal analysis. Reagents and calibration standards for nutrient analysis were prepared
162 using reagent grade chemicals.

163 **2.4 Laboratory incubation experiments**

164 The incubation studies were conducted with the samples from the riparian wetlands (Riparian 2 and
165 Riparian 1), the stream (Stream 2 and Stream 1) and the marsh wetlands (Marsh 1). The two locations in
166 riparian wetland soils and stream sediments had different total carbon, sulfur, and metal contents and
167 exhibited different solid-phase speciation of Cu. Both the locations in the marsh wetland soils showed
168 similar characteristics (Yan et al., 2021), so the samples from only one marsh wetland location (Marsh 1)
169 were used in further studies. Cu uptake experiments were performed to determine the Cu concentration
170 range to consider in the incubation studies. The soils and sediments were completely homogenized before
171 uptake experiments. These experiments were conducted in 15 mL polypropylene tubes containing 1-200
172 µM CuCl₂ and 10 mL of simulated site water, maintained at the desired pH (5.0 for Riparian 1 and Riparian

173 2, 7.6 for Stream 1 and Stream 2, and 7.0 for Marsh 1) and 0.5 g of soil/sediment. The recipe for the
174 simulated water included the major cations and anions analyzed in the water samples (Table S1 in the
175 Supplementary material). Samples were rotated end-over-end for 24 h to ensure complete mixing. After 4
176 h and 8 h of rotation, the pH values were readjusted to the original values, using 1M NaOH and 2M HCl
177 solutions. The suspension was then immediately filtered using disposable 0.22 μm MCE syringe filters and
178 acidified to 1% HNO_3 . Dissolved Cu concentrations were measured by ICP-MS (PerkinElmer, NexION
179 2000).

180 Incubation experiments were initiated under anaerobic conditions in 100 mL serum bottles
181 containing 2.5 g of homogenized soil/sediment along with 50 mL of simulated site water. The simulated
182 water only contained major cations and anions and lacked trace metals or Fe and Mn (Table S1). The pH
183 of the slurries was adjusted to 5.0 for Riparian 1 and Riparian 2, 7.6 for Stream 1 and Stream 2, and 7.0 for
184 Marsh 1, using NaOH and HCl solutions. For each site, three different conditions were studied: no Cu added
185 (control), low Cu loading, and high Cu loading (loading details are in Table 1). The different Cu loadings
186 were selected based on the Cu uptake experiments discussed above. The selection of loadings was done so
187 that the dissolved concentrations after 24 h of equilibration ranged between 10-100 nM and 100-2500 nM
188 for low and high Cu loadings, respectively (Figure 1). After 24 h of equilibration, 1 mM NO_3^- was added,
189 and the bottles were sealed with a 20 mm butyl stopper and aluminum cap. Immediately after the addition
190 of NO_3^- , 1 mL of the fluid was sampled to determine the concentrations of dissolved metals and nutrients.
191 The bottles were removed from the anaerobic chamber after NO_3^- addition and were flushed for 10 minutes
192 with ultrapure N_2 to remove trace amounts of O_2 and H_2 from the headspace.

193 To determine N_2O concentrations, headspace gas samples were taken from each serum bottle at 24
194 h intervals and were transferred to 3 mL pre-evacuated glass vials (Exetainer®, Labco, United Kingdom)
195 using a gas-tight syringe. The vials were stored upside down to prevent gas leakage from the septum. To
196 separate the dissolved phase, 1 mL of slurry from each serum bottle was sampled and centrifuged
197 (Spectrafuge 16M) for 5 min at 5000 rpm. The supernatant obtained was divided into three parts, 300 μL
198 was acidified to 1% HNO_3 for dissolved metal analysis, 400 μL was stored for nutrient analysis, and the

199 remaining supernatant was used to estimate the pH using Whatman pH indicator strips. At the end of
200 incubation experiments, the final pH value was recorded using a pH electrode. The water was filtered and
201 stored at 4°C to determine the dissolved organic carbon (DOC) concentration at the end of incubation
202 experiments.

203 **2.5 Analytical techniques used**

204 N₂O concentrations in the samples were measured using a gas chromatograph (GC) (Thermo Scientific GC
205 TRACE 1310). Specifically, 1000 µL of the gas sample was injected (split injection at the split rate of 10:1)
206 into the GC inlet (heated to 130 °C) using a TriPlus RSH (Thermo Scientific) autosampler equipped with a
207 2500 µL headspace syringe. The temperature of the column (Supelco Carboxen 1010 PLOT, 30 m x 0.32
208 mm) was maintained at 50 °C for 7.5 min, after which it was ramped to 130 °C using a rate of 20 °C/min
209 and then kept at this temperature for 2 min. Helium was used as the carrier gas at a flow rate of 30 mL/min.
210 A pulse discharge detector (PDD) at 150 °C was used for the analysis of N₂O. The concentration of the
211 standards varied from 10 ppmv to 0.1% N₂O and were prepared using a certified gas standard from Airgas.
212 The concentration of N₂O dissolved in the fluid was determined using the ideal gas law and Henry's gas
213 solubility law. The value of Henry's constant at 25 °C used for determining dissolved N₂O was 2.4×10^{-4}
214 mol m⁻³ Pa⁻¹ (Sander, 2015). The total N₂O present in the microcosm at the time of sampling was the sum
215 of the gas in the headspace and the gas dissolved in the water.

216 The dissolved metal concentrations (Cu, Fe, and Mn) were measured using inductively coupled
217 plasma mass spectrometer (PerkinElmer Elan DRC II). DOC concentrations were determined using a total
218 organic carbon analyzer (Shimadzu TOC-L). The nutrient concentrations (NO₃⁻, NO₂⁻ and NH₄⁺) were
219 obtained spectrophotometrically using a discrete multi-chemistry analyzer (Seal Analytical AQ300). The
220 samples used for nutrient analysis were frozen and then thawed overnight at 4°C before analysis. Nitrite
221 was measured by the reaction of the sample with sulfanilamide in dilute phosphoric acid to form a
222 diazonium compound which binds to N-(1-naphthyl)-ethylenediamine dihydrochloride to form an azo dye
223 detected at 520 nm (Huffman and Barbarick, 1981). To determine the nitrate concentration, NO₃⁻ was first

224 reduced to NO_2^- by cadmium and then the NO_2^- was measured. Ammonium present in the samples was
225 determined by reacting the samples with hypochlorite liberated from dichloroisocyanurate in an alkaline
226 solution followed by a reaction with salicylate in the presence of nitroferricyanide to form a blue indophenol
227 dye, which was measured at 660 nm (Krom, 1980).

228 **2.6 Complexation of dissolved Cu by DOC**

229 To estimate the speciation of Cu in the presence of organic carbon in the incubation experiments, the
230 nonideal competitive adsorption-Donnan (NICA-Donnan) model in Visual MINTEQ 3.1 (Yan and Korshin,
231 2014) was used. The model is a combination of NICA which enables simulation of metal complexation to
232 humic substances, and a Donnan model describing nonspecific electrostatic interactions between ions and
233 humic substances (Benedetti et al., 1995; Benedetti et al., 1996; Ren et al., 2015). Although humic
234 substances might not truly represent the dissolved organic matter present in aquatic systems (Kleber and
235 Lehmann, 2019; Myneni, 2019), we used the NICA-Donnan model to estimate the aqueous speciation of
236 Cu because this model has previously provided accurate predictions of metal speciation and availability in
237 natural systems (Han et al., 2014; Ponthieu et al., 2016). NICA considers competitive binding between
238 protons and metals to humic substances by accounting for binding site heterogeneity and ion-specific
239 nonideality (Benedetti et al., 1995). The generic parameters obtained in previous studies for Cu and proton
240 binding to humic material were used (Milne et al., 2001; Milne et al., 2003; Xu et al., 2016). Water
241 chemistry parameters (pH, total dissolved elements (Table S1)), dissolved Cu, Fe, and Mn, and dissolved
242 organic carbon (DOC) were used as the input parameters for determining dissolved Cu speciation. Three
243 sets of conditions were used to account for Cu speciation at different total dissolved Cu concentrations
244 corresponding to the control, low Cu loading, and high Cu loading experiments. The combined NICA-
245 Donnan model provides the amount of Cu bound to humic substances by using equations S1 and S2 shown
246 in supplementary material (details of the methodology and parameters used are provided in Section S1 and
247 Table S3). Under anoxic environments, as in our incubation experiments, Cu(II) can be reduced to Cu(I)
248 by microorganisms, inorganic reductants, and redox-active functional groups on dissolved organic matter

249 (Weber et al., 2006; Fulda et al., 2013b; Mehlhorn et al., 2018). Cu(I) can form stable complexes with
 250 inorganic ligands or thiol groups of organic matter (Yuan et al., 2012; Fulda et al., 2013b; Fulda et al.,
 251 2013a). In our speciation calculations, we have not accounted for the formation of these Cu(I)-thiol
 252 complexes, and dissolved Cu is assumed to be in Cu(II) form.

253 2.7 Kinetic model

254 A kinetic model was developed to quantify the effect of Cu on denitrification. Michaelis-Menten
 255 expressions were used to describe the evolution of NO_3^- , NO_2^- , N_2O , and N_2 during denitrification (Eq 1-
 256 4).

$$257 \quad \frac{d[\text{NO}_3^-]}{dt} = -V_{\max} \frac{[\text{C}_{\text{NO}_3^-}]}{K_{\text{NO}_3^-} + [\text{C}_{\text{NO}_3^-}]} \quad (1)$$

$$258 \quad \frac{d[\text{NO}_2^-]}{dt} = V_{\max} \left(\frac{[\text{C}_{\text{NO}_3^-}]}{K_{\text{NO}_3^-} + [\text{C}_{\text{NO}_3^-}]} - \frac{[\text{C}_{\text{NO}_2^-}]}{K_{\text{NO}_2^-} + [\text{C}_{\text{NO}_2^-}]} \right) - k_{\text{ab}}[\text{C}_{\text{NO}_2^-}] \quad (2)$$

$$259 \quad \frac{d[\text{N}_2\text{O}]}{dt} = V_{\max} \left(\frac{[\text{C}_{\text{NO}_2^-}]}{K_{\text{NO}_2^-} + [\text{C}_{\text{NO}_2^-}]} - \frac{[\text{C}_{\text{N}_2\text{O}}]}{K_{\text{N}_2\text{O}} + [\text{C}_{\text{N}_2\text{O}}]} \right) \quad (3)$$

$$260 \quad \frac{d[\text{N}_2]}{dt} = V_{\max} \left(\frac{[\text{C}_{\text{N}_2\text{O}}]}{K_{\text{N}_2\text{O}} + [\text{C}_{\text{N}_2\text{O}}]} \right) + k_{\text{ab}}[\text{C}_{\text{NO}_2^-}] \quad (4)$$

261 Here, V_{\max} denotes the maximum reaction rate under unlimited substrate supply ($\text{mmol-N L}^{-1} \text{ day}^{-1}$), C_y
 262 are the concentrations of N-containing species (mmol-N L^{-1}), and K_y values are Michaelis-Menten
 263 parameters (mmol-N L^{-1}) describing the substrate concentration at which the reaction rate is half V_{\max}
 264 (Bowman and Focht, 1974; Kremen et al., 2005). For model development, the concentration of N_2 was
 265 calculated from the mass balance on nitrogen species. As discussed earlier, abiotic nitrite reduction to N_2
 266 by inorganic electron donors, such as inorganic sulfur compounds (S^0 , S^{2-} , $\text{S}_2\text{O}_3^{2-}$), pyrite (FeS_2), thiocyanate
 267 (SCN^-), and ferrous ion (Fe^{2+}), is a pathway in N-cycling (Zhu and Getting, 2012; Zhu-Barker et al., 2015;
 268 Di Capua et al., 2019; Otte et al., 2019). Therefore an additional reaction, accounting for the abiotic
 269 reduction of NO_2^- to N_2 , was included in the model. A pseudo first-order reaction was used to define the
 270 abiotic reduction of NO_2^- in the system (incorporated in Eq 2 and 4), where k_{ab} (day^{-1}) is the pseudo first-

271 order rate constant assuming that the reductants are in excess (Matocha et al., 2012; Chen et al., 2020), and
272 $C_{\text{NO}_2^-}$ is the concentration of NO_2^- in the dissolved phase. Using the ODE45 function in MATLAB R2018a
273 (Shampine et al., 2003; Anyigor and Afiukwa, 2013), the unknown parameters were calculated. We
274 optimized the parameters and obtained the error estimates by minimizing the residuals using a non-linear
275 least-squares method. The value of V_{max} was determined using Eq 1 and data on the change in nitrate
276 concentration with time, and then the value was fixed to determine the rate parameters defined in Eq 2-4.
277 A constant value of V_{max} can be employed when organic carbon is present in excess of NO_3^- (Kremen et al.,
278 2005). The total organic carbon present in the systems studied far exceeded the amount of NO_3^- added
279 (Section S2 in SM). In separate optimizations in which we allowed the values of V_{max} to be different in
280 equations 1-4, the values were all in the narrow range of range 0.25 – 0.5 mmol-N L⁻¹ day⁻¹.

281 **3. Results**

282 **3.1 Characterization of soils and sediments**

283 Both the surface water samples, and the soils and sediments were characterized to determine their total
284 carbon, sulfur, metals, and nutrient concentrations. The detailed results are presented in our recent study
285 focused on trace metal micronutrient speciation in wetland soils and stream sediments (Yan et al., 2021).
286 The surface water in the marsh wetlands (Marsh 1) and stream sediments (Stream 1 and Stream 2) had pH
287 values ranging from 7.5-8.1, and they contained high concentrations of calcium, magnesium, and sulfate.
288 However, the riparian wetland surface water samples (Riparian 1 and Riparian 2) were at pH 5.5-6.0 with
289 substantially lower concentrations of major elements.

290 The mineralogy at all of the studied sites is dominated by quartz, with variations in minor phases (Yan
291 et al., 2021). The total organic carbon content of aquatic systems varies with location: the marsh wetland
292 site (Marsh 1) contained the highest carbon content (9.0%), whereas Stream 2 exhibited the lowest carbon
293 content (0.5%) (Table S2). The sulfur content was low at all sites (below 0.24%), following the trend Marsh
294 1 > Riparian 2 ≈ Stream 1 > Riparian 1 ≈ Stream 2. The total Fe concentration in the solid phases was
295 similar at all the sites (200 to 460 μmol/g), except for Riparian 1, which contained an order of magnitude

296 less Fe than the other soils/sediments. The concentration of Mn was two to three orders less than the Fe
297 content, with the highest values observed in stream sediments. Extractable ammonium in soils/sediments
298 was greater than extractable NO_3^- and NO_2^- at all the locations, which may indicate denitrification and/or
299 ammonium retention via cation exchange (Table S2).

300 **3.2 Selection of Cu loadings**

301 The total solid-phase concentrations of Cu were well below the crustal abundance (428 ± 61 nmol/g)
302 (Rudnick and Gao, 2003) at all the studied sites. The marsh wetland soil (Marsh 1) and Riparian 2
303 location in the riparian wetlands contained higher concentrations of solid-phase Cu than the other
304 locations. The dissolved Cu concentrations were less than 50 nM at the selected locations (Table 1),
305 indicating that Cu at these sites is predominantly associated with mineral and organic solid phases and
306 might not be bioavailable to microorganisms for N-cycling. Cu uptake experiments were used to
307 determine the Cu loadings to use in incubation experiments to target particular dissolved Cu
308 concentrations (Figure 1). The selected loadings resulted in dissolved Cu concentrations in the range of
309 15-300 nM and 50-2300 nM for low and high Cu amendments, respectively in the incubation experiments
310 (Table 1).

311 **3.3 Effect of Cu on evolution of nitrogen species concentrations during incubation**

312 The controls and the low-Cu amended sets showed similar NO_3^- reduction profiles in all the systems
313 studied (Figure 2). In controls and low-Cu amended systems, the complete reduction of 1 mM added NO_3^-
314 occurred within 16, 5, and 6 days for Riparian 2, Stream 1, and Marsh 1, respectively. In Riparian 1 and
315 Stream 2 experiments, complete reduction of NO_3^- did not occur, even after 27 days and 20 days of
316 incubation, respectively. A small delay in NO_3^- reduction after Cu addition was observed at high Cu loading
317 in Riparian 1, Riparian 2, and Stream 2 incubation experiments (Figure 2a, 2e, and 2m).

318 The presence of detectable NO_2^- was transient and showed a brief appearance followed by a rapid
319 decline in concentration in Riparian 2, Stream 1, and Marsh 1 incubations. In Riparian 1 soils, the dissolved

320 NO_2^- concentrations were below the detection limit ($0.0005 \text{ mmol-N L}^{-1}$) throughout the experiment,
321 suggesting rapid conversion of NO_2^- in these soils (Figure 2b). In the case of Riparian 2 and Stream 2
322 systems, Cu addition affected NO_2^- formation/reduction because more NO_2^- was detected in controls as
323 compared to Cu-amended sets.

324 For all the systems studied, less N_2O transiently accumulated in the sets amended with Cu. We did not
325 observe persistent accumulation of N_2O in the case of Riparian 1 soils (Figure 2c), however, the maximum
326 concentration of N_2O (control: $0.040 \text{ mmol-N L}^{-1}$ at 14 days, low-Cu: $0.032 \text{ mmol-N L}^{-1}$ at 10 days, and
327 high-Cu: $0.021 \text{ mmol-N L}^{-1}$ at 12 days) decreased as the dissolved Cu concentration increased. For Riparian
328 1 controls and low-Cu amended microcosms, N_2O started to accumulate after 3 days of incubation, whereas
329 in high-Cu amended sets, N_2O accumulation was only observed after 6 days of incubation. The complete
330 reduction of N_2O to N_2 was fast in low-Cu amended Riparian 1 sets; we did not observe N_2O after 14 days
331 in low-Cu added sets, whereas it took 29 and 23 days to completely reduce N_2O in high-Cu added and
332 control sets, respectively. In the Riparian 2 control, N_2O accumulated in the headspace and persisted until
333 the end of the experiment at 30 days, whereas the N_2O concentration first increased and then decreased
334 after 10 days and 16 days in Riparian 2 sets amended with low Cu and high Cu, respectively (Figure 2g).
335 For Riparian 2, relative to controls, the maximum N_2O concentration decreased by 38.6% in low Cu-added
336 sets and by 70.1% in high Cu-added sets. In the case of the stream sediments, Stream 1 showed a significant
337 effect of Cu addition on N_2O reduction; with respect to controls, the peak N_2O concentration decreased by
338 2.6 times and 7.8 times in sets with low and high Cu loading, respectively (Figure 2k). In Stream 2 and
339 Marsh 1 systems, we were able to measure detectable N_2O in the headspace of only the controls; in the Cu-
340 amended sets, any N_2O generated was rapidly reduced before the N_2O reached detectable levels (Figure 2n
341 and 2r).

342 The concentration of dissolved ammonium (NH_4^+) remained relatively constant throughout the
343 experiment for all the treatments (control, low loading, and high loading) in the systems studied (Figure 2).
344 Dissolved NH_4^+ was highest in Marsh 1, at $1.039 \pm 0.048 \text{ mmol-N/L}$. Riparian 2 and Riparian 1, contained
345 $0.130 \pm 0.004 \text{ mmol-N/L}$ and $0.033 \pm 0.004 \text{ mmol-N/L}$ NH_4^+ , respectively. The dissolved NH_4^+

346 concentrations in stream sediments averaged 0.053 ± 0.005 mmol-N/L and 0.172 ± 0.019 mmol-N/L in the
347 Stream 1 and Stream 2 samples, respectively.

348 **3.4 Variation in dissolved metal (Cu, Fe, and Mn) concentration**

349 Dissolved Cu, Fe, and Mn were monitored throughout the incubation experiments (Figure 3). The
350 dissolved Cu concentrations in the unamended control microcosms followed the trend Marsh 1 > Riparian
351 2 > Riparian 1 > Stream 2 > Stream 1. The dissolved Cu concentration remained relatively constant
352 throughout the experiment for Riparian 2, Stream 2, and Stream 1 experiments. However, a decrease in Cu
353 concentration was observed in all Riparian 1 sets, and controls and low-Cu amended Marsh 1 sets in the
354 initial days of incubation (Figure 3d and 3m).

355 A decrease in dissolved Fe concentration was observed during the experiment for the riparian
356 wetland soils (Riparian 1 and Riparian 2) and stream sediments (Stream 1 and Stream 2), whereas, in marsh
357 wetland soil (Marsh 1), dissolved Fe concentration did not fluctuate during the 8 days of incubation (Figure
358 3). In the Riparian 1 and Riparian 2 experiments, the dissolved Mn concentration remained constant and
359 was similar for all treatments (control, low and high Cu-loadings). However, in Stream 1 and Marsh 1, we
360 observed a decrease in the concentration of Mn until 7 days and 4 days, respectively and then it remained
361 constant (Figure 3i and 3o). Mn concentrations in Stream 2 experiments amended with high Cu were greater
362 than the concentrations in controls and low Cu-loading experiments (Figure 3l).

363 **3.5 Effect of Cu addition on denitrification rate**

364 The effect of Cu on denitrification was quantified with the help of the kinetic model. We obtained
365 Michaelis-Menten parameters (Table 2) and the abiotic rate constant for the set of differential equations
366 defined earlier (Eq 1-4). Here, $K_{NO_3^-}$, $K_{NO_2^-}$, and K_{N_2O} values reflect the ability of the microbial community
367 present in the soils and sediments to reduce NO_3^- to NO_2^- , NO_2^- to NO , and N_2O to N_2 , respectively under
368 the conditions studied. NO is rapidly transformed to N_2O , hence the conversion of NO to N_2O was assumed
369 to not be rate-limiting. The rate constant for abiotic reduction of NO_2^- to N_2 by inorganic donors in the

370 system is defined by k_{ab} , and inclusion of this reaction helped us reproduce the major features of all the
371 experiments (Figure 4). The abiotic reduction of NO_2^- to N_2O is also a possible pathway, but the
372 incorporation of this reaction into the kinetic model did not improve the fit to experimental data. Michaelis-
373 Menten parameters have an inverse relationship with rates, unlike rate constants; the smaller the value of
374 K_y , the faster the forward reaction; whereas the greater the value of k_{ab} , the faster the rate of abiotic nitrite
375 reduction. The model was able to describe the major features for nitrogen species reduction at all the sites
376 except for Marsh 1. For the Marsh 1 site, we observed a lag in NO_3^- reduction in all the incubation
377 experiments. Our model does not account for the acclimatization time of microorganisms after NO_3^- an
378 addition which could have caused poor fitting of data from the Marsh 1 experiments.

379 The modeled $K_{\text{NO}_3^-}$ values show that NO_3^- reduction is fastest in Stream 1 sediments followed by
380 Marsh 1, Riparian 2, Riparian 1, and Stream 2. The parameter $K_{\text{NO}_3^-}$ was similar for control and low Cu-
381 loading in all the systems studied. However, the modeled value increased (Table 2) in high Cu-loading sets
382 initiated with Riparian 1, Riparian 2, and Stream 2 sediments, indicating that the reduction of NO_3^- to NO_2^-
383 is slower in these sets amended with a high concentration of Cu.

384 Cu addition decreased NO_2^- accumulation in Riparian 2 and Stream 2 samples. The value of $K_{\text{NO}_2^-}$
385 was less in Cu-amended Riparian 2 experiments (control: $0.68 \text{ mmol-N L}^{-1}$; low Cu: $0.22 \text{ mmol-N L}^{-1}$; and
386 high Cu: $0.33 \text{ mmol-N L}^{-1}$), which signified that Cu enhanced the rate of NO_2^- reduction in Riparian 2 soils.
387 Similarly, in Stream 2 sediments, the modeled $K_{\text{NO}_2^-}$ values show a substantial decrease in Cu-amended
388 sets (control: $0.0079 \text{ mmol-N L}^{-1}$; low Cu: $0.0067 \text{ mmol-N L}^{-1}$; and high Cu: $0.0035 \text{ mmol-N L}^{-1}$).

389 The rate of N_2O to N_2 conversion, as indicated by the $K_{\text{N}_2\text{O}}$ parameter, increased upon Cu addition
390 in the Riparian 1, Riparian 2, Stream 1, and Stream 2 locations. In the marsh wetland soil, $K_{\text{N}_2\text{O}}$ remained
391 relatively constant in the control and Cu-amended experiments. The effect of Cu addition on N_2O reduction
392 was greatest in the Riparian 1 and Riparian 2 soils; in Riparian 2 soils, the value of $K_{\text{N}_2\text{O}}$ decreased from
393 $11000 \text{ mmol-N L}^{-1}$ in unamended control experiments to $0.48 \text{ mmol-N L}^{-1}$ and $0.21 \text{ mmol-N L}^{-1}$ in low-Cu
394 loading and high-Cu loading experiments, respectively. Similarly, in Riparian 1 soils, Cu addition increased

395 the N₂O conversion significantly; K_{N₂O} values decreased from 6900 mmol-N L⁻¹ to 24 mmol-N L⁻¹ and 3.5
396 mmol-N L⁻¹ at low and high Cu loadings, respectively.

397 The rate of abiotic NO₂⁻ to N₂ reduction was greater in Riparian 1 and Riparian 2 wetland soils than
398 in the other three systems; all microcosms incubated with Stream 2 sediments and Marsh 1 soils showed
399 negligible k_{ab} values. NO₂⁻ was not detected in any Riparian 1 incubation experiments (Figure 2b); the
400 abiotic rate constant for NO₂⁻ to N₂ reduction is high in Riparian 1 soils, which could have prevented NO₂⁻
401 accumulation in these soil incubations. The values of k_{ab} were similar for all the different incubation studies
402 (controls, low-Cu, and high-Cu loading) of a location, signifying that this step is not affected by the presence
403 of Cu.

404 **3.6 Labile concentration of Cu in soil/sediment incubations**

405 To understand Cu bioavailability as a nutrient and as a toxic element, we estimated the speciation of
406 dissolved Cu using Visual MINTEQ 3.1 and the NICA-Donnan model at the studied experimental
407 conditions and in the presence of dissolved organic carbon (Figure 5). The calculations predict that DOC
408 substantially decreased the lability of Cu in the systems studied. Here, the labile Cu concentration is defined
409 as the sum of Cu²⁺, Cu(OH)⁺, and Cu(OH)_{2(aq)}. In riparian wetland controls, Riparian 1 and Riparian 2, in
410 the studied pH range (5-6), Cu is predominantly present as Cu-organic matter complexes (Figure 6), and
411 the labile Cu concentration (Table S4), is < 3 nM. Similarly, in Stream 1 controls, the total labile Cu
412 concentration is < 1 nM in the experimental pH range (7.6-9.0). Due to a lower concentration of DOC in
413 Stream 2 (Figure 5), ~80% of dissolved Cu is present as labile Cu in Stream 2 controls. High DOC in Marsh
414 1 samples complexed ~84% of dissolved Cu(II), and only 7.6 nM remained as labile concentration in the
415 fluid of controls. In all the Cu-amended experiments, the lability of Cu was greater than the optimum
416 concentration (3-10 nM) determined to complete N₂O to N₂ conversion in pure culture studies and lake
417 systems (Granger and Ward, 2003; Twining et al., 2007). Additionally, in high-Cu amended experiments,
418 labile Cu in Riparian 1, Riparian 2, and Stream 2 was substantially higher (> 350 nM), which could inhibit

419 biological denitrification due to toxic effect (Allen and Hansen, 1996; Kozelka and Bruland, 1998; Huang
420 and Wang, 2003).

421 **4. Discussion**

422 **4.1 Role of labile Cu in nitrogen cycling**

423 The trends in nitrogen species transformation with and without Cu addition varied between different
424 sites as discussed in section 3.3. The labile concentration of Cu rather than the total dissolved concentration
425 helped us understand the evolution of nitrogen species at different sites. This study found that high dissolved
426 Cu concentrations decreased the rate of NO_3^- reduction in the riparian wetland soils (Riparian 1 and Riparian
427 2) and from the Stream 2 sediments. This observation is in line with previous results: higher concentrations
428 of Cu can inhibit denitrification by causing a shift in the community composition of denitrifiers (Magalhaes
429 et al., 2007; Wang et al., 2018; Zhao et al., 2020). A recent study that focused on evaluating the toxic effects
430 of copper oxide (CuO) nanoparticles on denitrification in soils observed that the Cu ions (Cu^{2+}) released
431 upon nanoparticle application can decrease nitrate reductase (Nar) activity by 21.1- 42.1%, causing an 11-
432 times decrease in NO_3^- reduction (Zhao et al., 2020). Elevated Cu^{2+} concentrations ($> 500 \mu\text{g g}^{-1}$ in solid-
433 phase and $\sim 0.95 \text{ mg L}^{-1}$ in dissolved form) can decrease biological denitrification by inhibiting extracellular
434 or intracellular enzymes (Fu and Tabatabai, 1989; Sakadevan et al., 1999; Ochoa-Herrera et al., 2011). At
435 high Cu loadings in the above-mentioned locations (Riparian 1, Riparian 2, and Stream 2), the labile Cu
436 concentrations estimated using the NICA-Donnan model were higher ($> 350 \text{ nM}$) than in Stream 1 (28 nM)
437 and Marsh 1 (150 nM) locations (Table S4), and the higher concentrations could have inhibited NO_3^-
438 reduction during the incubation experiments.

439 Incomplete reduction of NO_3^- was observed in incubation experiments using Riparian 1 soils and
440 Stream 2 sediments even when Cu was not added and had low labile concentrations. This suggests that
441 denitrification was limited by the low total organic carbon content at these sites (Ward et al., 2008). While
442 the total organic carbon present in the soils/sediments exceeded the amount stoichiometrically required for
443 complete reduction of NO_3^- (Section S2 in SM), not all of the organic carbon will be available to denitrifying

444 microorganisms (Schmidt et al., 2017). The biodegradability of the organic matter depends upon molecular
445 characteristics of the organic matter; carbohydrates, proteins, and organic acids are easily degradable,
446 whereas, aromatic and hydrophobic organic entities are recalcitrant to microbial activity (Marschner and
447 Kalbitz, 2003). The low degradability of organic matter is probably limiting NO_3^- reduction in Riparian 1
448 and Stream 2 sites. In future investigations the CO_2 respiration rate could be measured during the incubation
449 experiments to assess the association between organic matter oxidation and denitrification.

450 The dissolved Cu concentration in the Riparian 2 control (41 ± 9 nM) was higher than the optimum
451 concentration required for N_2O to N_2 conversion in pure culture studies (3 to 10 nM) (Granger and Ward,
452 2003; Twining et al., 2007; Glass and Orphan, 2012). However, N_2O accumulation was observed at the
453 Riparian 2 site, suggesting that the dissolved Cu may not have been completely bioavailable to the
454 microorganisms that convert N_2O to N_2 . The high DOC (47 mg C/L) at Riparian 2 (Figure 5) indicated the
455 presence of soluble organic ligands. These ligands may form soluble complexes with Cu, thus decreasing
456 Cu availability (Du Laing et al., 2009; Zhang et al., 2014). The free Cu^{2+} and the Cu(II)-hydroxo complexes
457 concentrations control the bioavailability of Cu rather than the total dissolved concentration (Black et al.,
458 2011; Bourgeault et al., 2013). The labile Cu concentration in Riparian 2 control experiments, shown as
459 the sum of Cu^{2+} , $\text{Cu}(\text{OH})^+$, and $\text{Cu}(\text{OH})_{2(\text{aq})}$ (Table S4), is ~ 1.4 nM which is less than the optimum Cu
460 concentration (3-10 nM) (Granger and Ward, 2003; Twining et al., 2007; Glass and Orphan, 2012) required
461 for conversion of N_2O to N_2 in pure culture studies. Thus, the low lability of Cu in Riparian 2 control sets
462 could have caused persistent N_2O accumulation in the headspace.

463 In Riparian 1 soils, both the background dissolved Cu concentration (29.3 nM) and the solid-phase-
464 associated Cu (48.3 nmol/g) were less than the Cu concentration in Riparian 2 soils (dissolved: 41 nM;
465 solid-phase: 262.3 nmol/g), but N_2O did not accumulate persistently in the headspace of Riparian 1 soils.
466 This observation suggests that bioavailable Cu for N_2O to N_2 conversion is more abundant in Riparian 1
467 soils. Riparian 1 soils have less dissolved organic carbon (23 mg C/L) than Riparian 2 soils, and thus are
468 less able to decrease the bioavailability of Cu by forming soluble complexes of organic matter with Cu. The
469 speciation results corroborated the hypothesis because in the pH range studied, the dissolved labile Cu in

470 Riparian 1 controls (2.8 ± 0.9 nM) was greater than Riparian 2 controls (1.4 ± 0.8 nM). Prior study on a
471 lake system indicated that the presence of 3 nM dissolved Cu decreased N_2O accumulation during
472 denitrification relative to systems containing no Cu (Twining et al., 2007). Although the rate of N_2O to N_2
473 conversion was slow in Riparian 1 controls as compared to Cu-amended sets (Table 2), the labile-Cu
474 concentration closer to optimum range (3-10 nM) prevented persistent N_2O accumulation in the headspace.

475 The concentration of accumulated N_2O in the headspace of Stream 1 controls was greater than the
476 Stream 2 controls. Both stream sediment sites contained low concentrations of dissolved Cu in the control
477 sets (3.1 ± 1 nM at Stream 1, and 6.2 ± 1.9 nM at Stream 2), however, substantial N_2O accumulation was
478 only observed at Stream 1 location. This finding suggests that the low Cu concentrations of ~ 6 nM were
479 sufficient to enable the N_2O to N_2 conversion in Stream 2 sediments. The dissolved organic carbon
480 concentration is lower at the Stream 2 location (2.1 mg C/L, Figure 5) which indicated that the fraction of
481 dissolved Cu that is labile (i.e., not complexed with organic ligands) would be higher for Stream 2 (labile
482 Cu in Stream 1: 0.55 nM and Stream 2: 4.8 nM). Thus, the presence of un-complexed Cu(II) at a
483 concentration of ~ 4.8 nM enabled N_2O to N_2 conversion in Stream 2 controls.

484 N_2O was not detected in the headspace of Marsh 1 Cu-amended microcosms, however, we observed
485 accumulation of N_2O in unamended control experiments in the initial days of incubation (max N_2O : 0.064
486 mmol-N/L). This observation suggests that the rate of N_2O to N_2 conversion was promoted by Cu
487 amendment in Marsh 1 site (Figure 2s). The dissolved Cu concentration in the control samples was 48 nM,
488 which is higher than the optimal range (3 to 10 nM) for N_2O transformation in pure culture studies (Granger
489 and Ward, 2003; Glass and Orphan, 2012). The dissolved organic carbon (32 mg C/L) at the site is
490 calculated to have decreased the bioavailability of Cu substantially (labile Cu in controls: 7.6 ± 5 nM) in
491 the pH range studied, thus resulting in the transient N_2O accumulation in the headspace of the unamended
492 controls.

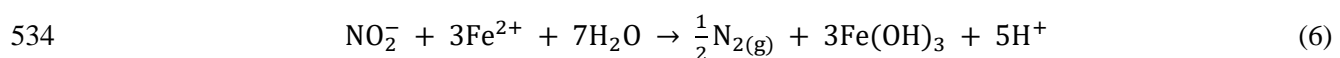
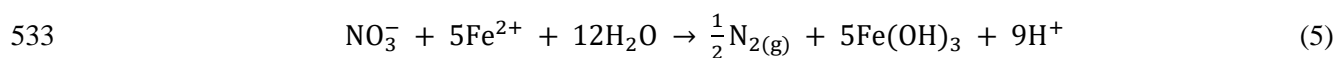
493 **4.2 Ammonium release during the incubations**

494 In all the locations studied, a substantial amount of NH_4^+ was detected in the dissolved phase and
495 remained constant throughout the experiment (Figure 2). Exchangeable NH_4^+ can be released from the solid
496 phase to the fluid because of changes in the water-to-solid ratio, pH, and ionic strength. Alternatively, the
497 NH_4^+ can result from the microbially-mediated dissimilatory nitrate reduction to ammonium (DNRA)
498 (Wang et al., 2008; Robertson and Thamdrup, 2017; Zhu et al., 2019; Liu et al., 2020; Wang et al., 2020).
499 The ammonium was released into the fluid phase even before the onset of NO_3^- reduction (Figure 2), and
500 the concentration of NH_4^+ remained constant throughout the experiment. This observation indicated that
501 most of the released NH_4^+ was due to exchange from the soils/sediments and not due to biological nitrate
502 reduction. Additionally, the mass balance of extractable ammonium in soils/sediments indicates that the
503 soils/sediments have the capacity to release the amounts of NH_4^+ observed in the fluid (Riparian 1: 0.05
504 mmol-N L^{-1} , Riparian 2: 0.14 mmol-N L^{-1} , Stream 1: 0.15 mmol-N L^{-1} , Stream 2: 0.14 mmol-N L^{-1} , and
505 Marsh 1: 1.04 mmol-N L^{-1}).

506 **4.3 Relationship between pH, dissolved metal content, and denitrification**

507 During the initial 2-3 days of incubation, the pH increased from 5.0 to ~ 6.5 for Riparian 1 and Riparian
508 2 soils, from 7.6 to ~ 8.9 for Stream 1 and Stream 2 sediments, and from 7.0 to ~ 8.2 for Marsh 1 soils, and
509 then remained relatively constant. The increase in pH values can be attributed to NO_3^- and NO_2^- reduction
510 during denitrification. Previous study on riparian soils indicated that the pH increased from 5 to 7 and 5 to
511 9 in unbuffered NO_3^- reduction experiments with low ($111 \mu\text{mol N g}^{-1}$) and high ($500 \mu\text{mol N g}^{-1}$) nitrogen
512 loadings, respectively (Clement et al., 2005). In contrast, pH variation was limited (± 0.5) when
513 denitrification occurred in carbonate-buffered lowland soils from Northern Italy (Castaldelli et al., 2019).
514 Our previous study on the studied natural aquatic systems indicated that these soils and sediments lacked
515 carbonate minerals (Yan et al., 2021); hence, the buffering capacity of the soils/sediments was likely
516 inadequate to prevent the increase in pH upon NO_3^- and NO_2^- reduction.

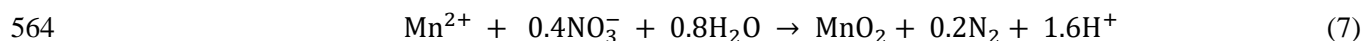
517 The dissolved concentrations of Cu, Fe, and Mn were indirectly affected by nitrogen cycling in the
 518 incubation experiments. Due to a pH increase driven by denitrification, adsorption of metals to minerals
 519 phases increased and caused the dissolved concentrations of Cu, Fe, and Mn to decrease with time (Schultz
 520 and Grundl, 2004; Zhang et al., 2014) . The decrease in Cu concentrations in Riparian 1 systems and
 521 controls and low-Cu amended sets of Marsh 1 soils (Figure 3a, 3d and 3m) likely resulted from an increase
 522 in Cu adsorption with increasing pH. We also observed that substantial amounts of Fe and Mn were released
 523 into the water in all of the incubation experiments after 24 h of incubation, indicating the reductive
 524 dissolution of Fe/Mn oxyhydroxides under anaerobic conditions (Zhang et al., 2014). The change in the
 525 ionic strength and pH of the soils/sediments during the preparation of the slurries could have also caused
 526 dispersion of colloidal Fe and Mn (Seta and Karathanasis, 1996). The released Fe decreased over time in
 527 the Riparian 1, Riparian 2, Stream 1, and Stream 2 sites. Under the conditions studied, dissolved Fe
 528 predominantly exists as Fe(II); the extent of Fe(II) sorption on clays, silica, and metal-oxide phases
 529 increases with an increase in pH (Schultz and Grundl, 2004; Nano and Strathmann, 2006; Zhu and Elzinga,
 530 2014). Additionally, Fe(II) may serve as an electron donor for the abiotic reduction of NO_3^- and NO_2^- to
 531 form N_2 in soils and sediments (Eq 5-6) (Burgin and Hamilton, 2007; Klueglein et al., 2014; Robertson and
 532 Thamdrup, 2017; Liu et al., 2019; Otte et al., 2019; Rahman et al., 2019; Robinson et al., 2021).



535 Although the abiotic reduction of NO_3^- to N_2 in the presence of Fe(II) is thermodynamically feasible,
 536 studies indicate that NO_3^- can only be directly reduced by Fe(II) in the presence of mixed-valence Fe-
 537 bearing solids (green-rusts), or a catalyst, such as Cu(II), Sn(II), and Ag(I) (Moraghan and Buresh, 1977;
 538 Ottley et al., 1997; Davidson et al., 2003). Fe(II) adsorbed to iron-oxide surfaces is a stronger reducing
 539 agent than Fe(II) in dissolved form (Stumm and Sulzberger, 1992; Davidson et al., 2003), hence adsorbed
 540 Fe(II) might promote NO_3^- reduction in the studied systems. Additionally, biological oxidation of structural
 541 Fe(II) in clay minerals, such as illite and nontronite, can be coupled with reduction of NO_3^- to N_2 (Zhao et

542 al., 2013; Zhao et al., 2017). In our incubation studies, the dissolved Fe concentration decreased until 27,
543 18, and 6 days in Riparian 1, Riparian 2, and Stream 1 systems, respectively and then remained almost
544 constant through the end of the experiments. Decreases in Fe concentration were only observed until the
545 $\text{NO}_3^-/\text{NO}_2^-$ were completely consumed in these systems indicating that Fe(II) oxidation to Fe(III)
546 oxides/hydroxides is coupled abiotically or biotically to $\text{NO}_3^-/\text{NO}_2^-$ reduction at Riparian 1, Riparian 2, and
547 Stream 1 sites. Mass balance calculations indicated that NO_3^- concentrations were sufficient to allow for
548 consumption of Fe(II) in Riparian 1, Riparian 2, and Stream 1 systems to react with Fe(II) (Section S3 in
549 SM). The values of k_{ab} relative to $K_{\text{NO}_2^-}$ were high in Riparian 1, Riparian 2, and Stream 1 systems,
550 suggesting that the reaction involving abiotic NO_2^- reduction is substantial in these systems. On the other
551 hand, the decrease in the Fe(II) concentration in Stream 2 experiments aligned with the pH increase during
552 the initial 2-3 days of incubation, so the decrease in Fe concentration could also be due to increased
553 adsorption at higher pH.

554 The addition of Cu affected Mn concentrations in Stream 2 experiments; the release of Mn was
555 greater in sets amended with high Cu (Figure 3l). In stream 2 incubation experiments with high Cu loading,
556 250 μM Cu was added and only 0.60 μM remained in the dissolved phase after 24 h equilibration; the
557 competitive adsorption of Cu(II) onto active sites of mineral-phases could have mobilized Mn(II) (~ 40 μM
558 in this case) to the water. Prior studies have also observed the release of Mn(II) in the presence of Cu due
559 to competitive adsorption (Kurdi and Donner, 1983; Traina and Doner, 1985). In Stream 1 and Marsh 1
560 studies, the concentration of dissolved Mn decreased with time (Figure 3i and 3o). Mn adsorption has been
561 found to increase with pH on clay minerals, iron oxides/hydroxides and aluminum oxides. In reducing NO_3^- ,
562 Mn^{2+} can also serve as an electron donor (Eq 7) to autotrophic denitrifiers belonging to the genera
563 *Acinetobacter* and *Pseudomonas* (Su et al., 2015; Su et al., 2016).



565 Thus, the decrease in the concentration of Mn observed in Stream 1 and Marsh 1 samples can result from
566 increased adsorption caused by a shift in pH or from Mn consumption by autotrophic denitrifiers.

567 **4.4 Comparison of nitrogen cycling with materials from different systems**

568 The studied aquatic systems, even different locations of the same site, showed varied trends in the
569 reduction of nitrogen species in the incubation experiments. The total dissolved Cu concentrations in both
570 locations of EFPC stream sediments (Stream 1 and Stream 2) were very low (3-10 nM), but transient N₂O
571 accumulation only occurred in their unamended controls, whereas TB riparian wetland soils (Riparian 1
572 and Riparian 2) showed substantial N₂O accumulation despite having much higher dissolved background
573 Cu concentrations of 30-50 nM. This disparity suggests that the speciation of Cu, and hence its
574 bioavailability, plays a more important role than the total Cu content in controlling N₂O to N₂ conversion
575 in the studied environmental systems.

576 Even after Cu addition, the accumulated concentrations of N₂O in the riparian wetland samples
577 were higher than in the other locations. One possible explanation is that the riparian wetland incubation
578 experiments were conducted at pH 5, whereas the incubations for marsh wetland soils (Marsh 1) and stream
579 sediments (Stream 1 and Stream 2) were performed at neutral pH conditions. Acidic soils decrease the
580 activity of the nitrous oxide reductase enzyme, leading to N₂O accumulation (Knowles, 1982; Simek and
581 Cooper, 2002; Pan et al., 2012; Carreira et al., 2020). Optimal N₂O reduction has been observed in the pH
582 range of 7.5-8.0; previous studies have observed substantial N₂O accumulation in the pH range of 6.0-6.5
583 (Pan et al., 2012; Carreira et al., 2020). Although the pH in the riparian wetland soils increased to ~ 6.5 in
584 the first two days of incubation, i.e., before the onset of N₂O accumulation, it was in the range where a
585 decrease in the activity of nitrous reductase enzyme has been observed (Pan et al., 2012; Carreira et al.,
586 2020). Thus, Riparian 1 and Riparian 2 wetland soils could be a significant source of N₂O, not only because
587 the bioavailable Cu is limited but also because they are acidic.

588 **5. Geochemical significance and implications**

589 Most pristine natural aquatic systems contain low solid-phase Cu, and hence they may have low
590 availability of Cu for microbial denitrification. The limited set of studies on natural aquatic systems
591 containing Cu at concentrations less than or equal to crustal abundances (441±63 nmol g⁻¹) support our

592 major finding that increased Cu concentrations can increase the extent of conversion of N₂O to N₂. At 26
593 μM dissolved Cu, Giannopoulos et al. (2020) concluded that greater availability of Cu led to less N₂O
594 accumulation and higher abundance of Cu-dependent enzymes in wetland soils. A study on agricultural
595 soils indicated that the application of organic fertilizer modified with 130 mM CuSO₄ decreased N₂O
596 emissions substantially (Shen et al., 2020). However, these above-mentioned studies evaluated Cu
597 concentrations that are relatively higher than the optimum range (3-10 nM) required for N₂O to N₂
598 transformation in pure culture studies. The concentrations of dissolved Cu in natural environments are
599 typically low (< 200 nM), and the presence of inorganic/organic ligands can further decrease the
600 bioavailability of Cu causing incomplete denitrification with N₂O accumulation. Our results indicated that
601 without Cu amendment, substantial N₂O accumulation can take place in soils and sediments.

602 The selected sites represent different aquatic systems in geologically-distinct regions and contain low
603 solid-phase and dissolved Cu (solid-phase: 45-280 nmol g⁻¹ and dissolved: 3-48 nM). Despite the differences
604 in mineralogy, elemental composition, and aqueous-phase characteristics, the presence of dissolved Cu at
605 trace levels (10-500 nM) decreased N₂O accumulation in all the sites. The response of riparian wetland
606 soils (Riparian 1 and Riparian 2) to Cu addition was less pronounced than that of other studied sites, which
607 highlights that that the systems with acidic conditions like Riparian 1 and 2 can be substantial contributors
608 of N₂O emissions even in the abundance of Cu.

609 Our study provides greater insight into the importance of Cu speciation on cycling of nitrogen species
610 in environmental systems. The effect of Cu on N₂O accumulation was more closely associated with
611 estimated labile-Cu concentrations than with total dissolved Cu concentrations. Dissolved Cu in the
612 porewater of soils and sediments was substantially lower than the total solid-phase associated concentration,
613 and its lability is lowered by its interactions with dissolved organic matter (Bourgeault et al., 2013; Zhang
614 et al., 2014).

615 For systems with Cu limitations of complete denitrification, our results indicate that the addition of
616 minor amounts of Cu can increase the rate of N₂O conversion in natural aquatic systems. Natural soils have
617 been recognized as an important source of N₂O to the atmosphere and are estimated to release up to 5.6 Tg

618 N₂O-N yr⁻¹ (Tian et al., 2020). Current ecosystem models, such as DLEM, incorporate multiple
619 environmental factors, including moisture content, temperature, nitrate and dissolved organic carbon
620 concentration, and pH, in the estimation of N₂O emissions from terrestrial systems (Tian et al., 2015). These
621 models do not account for the effect of trace metal micronutrient availability (Cu, Ni, Zn, Co, and Mo) on
622 biogeochemical processes responsible for the release of greenhouse gas emissions. The inclusion of Cu as
623 an additional parameter can help improve the accuracy of existing ecosystem models to predict N₂O
624 emissions from soils and sediments. Addition of Cu at micronutrient levels to natural aquatic systems could
625 potentially decrease N₂O release to the atmosphere. Addition of CuSO₄ in lakes is commonly practiced to
626 inhibit algal growth. Previous studies indicate that Cu concentrations above 100 nM can decrease algal and
627 bacterial populations in surface waters (Flemming and Trevors, 1989). Hence, addition of Cu at
628 micronutrient levels (10-30 nM) is not expected to be toxic to aquatic organisms. Changes in Cu speciation
629 in wetlands and stream sediments associated with hydrologic variation could also influence net N₂O
630 emissions.

631 **6. Conclusions**

632 Through a combination of incubation experiments and a kinetic model we determined the effect of dissolved
633 Cu at trace levels (10-500 nM) on the rate of N₂O reduction. Only the systems containing estimated labile
634 Cu < 10 nM had substantial N₂O accumulation. Even with a small increase in dissolved Cu concentration,
635 as observed in low-Cu-loaded incubation experiments, the rate of N₂O to N₂ conversion was significantly
636 enhanced. The contribution of the abiotic reduction of NO₂⁻ to N₂ by Fe(II) was significant at Riparian 1,
637 Riparian 2, and Stream 1 locations. Riparian wetland soils showed higher N₂O accumulation than the other
638 sites studied, indicating that the acidic pH conditions can enhance N₂O emissions from natural
639 environments. The sites containing high concentrations of DOC (Riparian 1, Riparian 2, and Marsh 1) had
640 less concentrations of dissolved Cu that were labile and showed greater N₂O accumulation. Our results
641 indicate that including Cu bioavailability in ecosystem models could improve the accuracy of estimates of
642 N₂O emissions from natural landscapes.

643 **Acknowledgements**

644 This project was supported by the U.S. Department of Energy, Office of Science, Office of Biological and
645 Environmental Research, Subsurface Biogeochemical Research program through award no. DE-
646 SC0019422 to Washington University. We acknowledge our collaborators, Pamela Weisenhorn, Edward J.
647 O’Loughlin, and Kenneth M. Kemner at Argonne National Laboratory, Grace E. Schwartz and Scott C.
648 Brooks at Oak Ridge National Laboratory, and Daniel I. Kaplan at Savannah River National Laboratory,
649 who helped us in collecting samples from the selected aquatic systems. We thank Jinshu Yan, a doctoral
650 student in the Department of Earth and Planetary Sciences for characterizing the soils/sediments used for
651 the incubation experiments. ICP-MS measurements were performed in the Nano Research Facility (NRF)
652 at Washington University in St. Louis. We also thank the McDonnell International Scholars Academy for
653 the fellowship that is supporting Neha Sharma in her graduate program. We also thank James Ballard for
654 assisting us in improving the quality of writing in this manuscript.

655 **Appendix A. Supplementary Material**

656 The supplementary material includes information on the recipe of the simulated water used for Cu uptake
657 and incubation experiments, concentrations of solid-phase associated metals and nutrients, methodology
658 and parameters used for estimating Cu speciation in the presence of dissolved organic carbon, the
659 concentration of estimated labile Cu using NICA-Donnan model, and the calculations showing organic
660 matter and Fe(II) requirements for nitrate reduction during the incubation experiments.

661 **Research Data**

662 Data associated with this article can be accessed at <https://data.mendeley.com/datasets/t359pdpcxy/1>.

663 **References**

- 664 Allen H. E. and Hansen D. J. (1996) The importance of trace metal speciation to water quality criteria.
665 *Water Environ. Res.* **68**, 42–54.
- 666 Anyigor C. and Afiukwa J. (2013) Application of matlab ordinary differential equation function solver
667 (ode45) in modelling and simulation of batch reaction kinetics. *Am. J. Sci. Ind. Res.* **4**, 285–287.
- 668 Baeseman J. L., Smith R. L. and Silverstein J. (2006) Denitrification potential in stream sediments
669 impacted by acid mine drainage: Effects of pH, various electron donors, and iron. *Microb. Ecol.* **51**,
670 232–241.
- 671 Benedetti M. F., Milne C. J., Kinniburgh D. G., Van Riemsdijk W. H. and Koopal L. K. (1995) Metal ion
672 binding to humic substances: Application of the non-ideal competitive adsorption model. *Environ.*
673 *Sci. Technol.* **29**, 446–457.
- 674 Benedetti M. F., Van Riemsdijk W. H. and Koopal L. K. (1996) Humic substances considered as a
675 heterogeneous Donnan gel phase. *Environ. Sci. Technol.* **30**, 1805–1813.
- 676 Bertero M. G., Rothery R. A., Palak M., Hou C., Lim D., Blasco F., Weiner J. H. and Strynadka N. C. J.
677 (2003) Insights into the respiratory electron transfer pathway from the structure of nitrate reductase
678 *A. Nat. Struct. Biol.* **10**, 681–687.
- 679 Black A., Hsu P. C. L., Hamonts K. E., Clough T. J. and Condrón L. M. (2016) Influence of copper on
680 expression of nirS, norB and nosZ and the transcription and activity of NIR, NOR and N2OR in the
681 denitrifying soil bacteria *Pseudomonas stutzeri*. *Microb. Biotechnol.* **9**, 381–388.
- 682 Black A., McLaren R. G., Reichman S. M., Speir T. W. and Condrón L. M. (2011) Evaluation of soil
683 metal bioavailability estimates using two plant species (*L. perenne* and *T. aestivum*) grown in a
684 range of agricultural soils treated with biosolids and metal salts. *Environ. Pollut.* **159**, 1523–1535.
- 685 Bourgeault A., Ciffroy P., Garnier C., Cossu-Leguille C., Masfarau J. F., Charlatchka R. and Garnier J.
686 M. (2013) Speciation and bioavailability of dissolved copper in different freshwaters: Comparison
687 of modelling, biological and chemical responses in aquatic mosses and gammarids. *Sci. Total*
688 *Environ.* **452–453**, 68–77.
- 689 Bowman R. A. and Focht D. D. (1974) The influence of glucose and nitrate concentrations upon
690 denitrification rates in sandy soils. *Soil Biol. Biochem.* **6**, 297–301.
- 691 Brown K., Tegoni M., Prudêncio M., Pereira A. S., Besson S., Moura J. J., Moura I. and Cambillau C.
692 (2000) A novel type of catalytic copper cluster in nitrous oxide reductase. *Nat. Struct. Biol.* **7**, 191–
693 195.
- 694 Bruland K. W., Rue E. L., Donat J. R., Skrabal S. A. and Moffett J. W. (2000) Intercomparison of
695 voltammetric techniques to determine the chemical speciation of dissolved copper in a coastal

696 seawater sample. *Anal. Chim. Acta* **405**, 99–113.

697 Buchwald C., Grabb K., Hansel C. M. and Wankel S. D. (2016) Constraining the role of iron in
698 environmental nitrogen transformations: Dual stable isotope systematics of abiotic NO₂- reduction
699 by Fe(II) and its production of N₂O. *Geochim. Cosmochim. Acta* **186**, 1–12.

700 Burgin A. J. and Hamilton S. K. (2007) Have we overemphasized the role of denitrification in aquatic
701 ecosystems? A review of nitrate removal pathways. *Front. Ecol. Environ.* **5**, 89–96.

702 Campana O., Simpson S. L., Spadaro D. A. and Blasco J. (2012) Sub-lethal effects of copper to benthic
703 invertebrates explained by sediment properties and dietary exposure. *Environ. Sci. Technol.* **46**,
704 6835–6842.

705 Di Capua F., Pirozzi F., Lens P. N. L. and Esposito G. (2019) Electron donors for autotrophic
706 denitrification. *Chem. Eng. J.* **362**, 922–937.

707 Carreira C., Nunes R. F., Mestre O., Moura I. and Pauleta S. R. (2020) The effect of pH on *Marinobacter*
708 *hydrocarbonoclasticus* denitrification pathway and nitrous oxide reductase. *J. Biol. Inorg. Chem.* **25**,
709 927–940.

710 Castaldelli G., Colombani N., Soana E., Vincenzi F., Fano E. A. and Mastrocicco M. (2019) Reactive
711 nitrogen losses via denitrification assessed in saturated agricultural soils. *Geoderma* **337**, 91–98.

712 Chakraborty P., Ramteke D. and Chakraborty S. (2015) Geochemical partitioning of Cu and Ni in
713 mangrove sediments: Relationships with their bioavailability. *Mar. Pollut. Bull.* **93**, 194–201.

714 Chen D., Yuan X., Zhao W., Luo X., Li F. and Liu T. (2020) Chemodenitrification by Fe(II) and nitrite:
715 pH effect, mineralization and kinetic modeling. *Chem. Geol.* **541**, 119586.

716 Clement J. C., Shrestha J., Ehrenfeld J. G. and Jaffe P. R. (2005) Ammonium oxidation coupled to
717 dissimilatory reduction of iron under anaerobic conditions in wetland soils. *Soil Biol. Biochem.* **37**,
718 2323–2328.

719 Davidson E. A., Chorover J. and Dail D. B. (2003) A mechanism of abiotic immobilization of nitrate in
720 forest ecosystems: The ferrous wheel hypothesis. *Glob. Chang. Biol.* **9**, 228–236.

721 Doane T. A. (2017) The Abiotic Nitrogen Cycle. *ACS Earth Sp. Chem.* **1**, 411–421.

722 Doroski A. A., Helton A. M. and Vadas T. M. (2019) Greenhouse gas fluxes from coastal wetlands at the
723 intersection of urban pollution and saltwater intrusion: A soil core experiment. *Soil Biol. Biochem.*
724 **131**, 44–53.

725 Flemming C. A. and Trevors J. T. (1989) Copper toxicity and chemistry in the environment: a review.
726 *Water. Air. Soil Pollut.* **44**, 143–158.

727 Fu M. H. and Tabatabai M. A. (1989) Nitrate reductase activity in soils: Effects of trace elements. *Soil*
728 *Biol. Biochem.* **21**, 943–946.

729 Fulda B., Voegelin A., Ehlert K. and Kretzschmar R. (2013a) Redox transformation, solid phase

730 speciation and solution dynamics of copper during soil reduction and reoxidation as affected by
731 sulfate availability. *Geochim. Cosmochim. Acta* **123**, 385–402.

732 Fulda B., Voegelin A., Maurer F., Christl I. and Kretzschmar R. (2013b) Copper redox transformation
733 and complexation by reduced and oxidized soil humic acid. 1. X-ray absorption spectroscopy study.
734 *Environ. Sci. Technol.* **47**, 10903–10911.

735 Giannopoulos G., Hartop K. R., Brown B. L., Song B., Elsgaard L. and Franklin R. B. (2020) Trace metal
736 availability affects Greenhouse Gas emissions and microbial functional group abundance in
737 freshwater wetland sediments. *Front. Microbiol.* **11**, 1–12.

738 Glass J. B. and Orphan V. J. (2012) Trace metal requirements for microbial enzymes involved in the
739 production and consumption of methane and nitrous oxide. *Front. Microbiol.* **3**, 1–20.

740 Godden A. J. W., Turley S., Teller D. C., Adman E. T., Liu M. Y., Payne W. J. and Legall J. (1991) The
741 2.3 angstrom X-Ray structure of nitrite reductase from *Achromobacter cycloclastes*. *Science (80-.)*.
742 **253**, 438–442.

743 Granger J. and Ward B. B. (2003) Accumulation of nitrogen oxides in copper-limited cultures of
744 denitrifying bacteria. *Limnol. Oceanogr.* **48**, 313–318.

745 Han S., Zhang Y., Masunaga S., Zhou S. and Naito W. (2014) Relating metal bioavailability to risk
746 assessment for aquatic species: Daliao River watershed, China. *Environ. Pollut.* **189**, 215–222.

747 Huang S. and Wang Z. (2003) Application of anodic stripping voltammetry to predict the
748 bioavailable/toxic concentration of Cu in natural water. *Appl. Geochemistry* **18**, 1215–1223.

749 Huffman S. A. and Barbarick K. A. (1981) Soil nitrate analysis by cadmium reduction. *Commun. Soil Sci.*
750 *Plant Anal.* **12**, 79–89.

751 IPCC (2014) Climate Change 2014: Impacts, Adaptation, and Vulnerability. Contribution of Working
752 Group II to the Fifth Assessment Report of the Intergovernmental Panel on Climate Change.

753 Iwasaki H., Saigo T. and Matsubara T. (1980) Copper as a controlling factor of anaerobic growth under
754 N₂O and biosynthesis of N₂O reductase in denitrifying bacteria. *Plant Cell Physiol.* **21**, 1573–1584.

755 Jacinthe P. A. and Tedesco L. P. (2009) Impact of elevated copper on the rate and gaseous products of
756 denitrification in freshwater sediments. *J. Environ. Qual.* **38**, 1183–1192.

757 Jormakka M., Richardson D., Byrne B. and Iwata S. (2004) Architecture of NarGH reveals a structural
758 classification of Mo-bisMGD enzymes. *Structure* **12**, 95–104.

759 Kleber M. and Lehmann J. (2019) Humic substances extracted by alkali are invalid proxies for the
760 dynamics and functions of organic matter in terrestrial and aquatic ecosystems. *J. Environ. Qual.* **48**,
761 207–216.

762 Klueglein N., Zeitvogel F., Stierhof Y. D., Floetenmeyer M., Konhauser K. O., Kappler A. and Obst M.
763 (2014) Potential role of nitrite for abiotic Fe(II) oxidation and cell encrustation during nitrate

764 reduction by denitrifying bacteria. *Appl. Environ. Microbiol.* **80**, 1051–1061.

765 Knowles R. (1982) Denitrification. *Microbiol. Rev.* **46**, 43–70.

766 Koponen H. T., Flojt L. and Martikainen P. J. (2004) Nitrous oxide emissions from agricultural soils at
767 low temperatures: A laboratory microcosm study. *Soil Biol. Biochem.* **36**, 757–766.

768 Kozelka P. B. and Bruland K. W. (1998) Chemical speciation of dissolved Cu, Zn, Cd, Pb in Narragansett
769 Bay, Rhode Island. *Mar. Chem.* **60**, 267–282.

770 Kremen A., Bear J., Shavit U. and Shaviv A. (2005) Model demonstrating the potential for coupled
771 nitrification denitrification in soil aggregates. *Environ. Sci. Technol.* **39**, 4180–4188.

772 Krom M. D. (1980) Spectrophotometric determination of ammonia: a study of a modified Berthelot
773 reaction using salicylate and dichloroisocyanurate. *Analyst* **105**, 305–316.

774 Kurdi F. and Donner H. E. (1983) Zinc and Copper Sorption and Interaction in Soils. *Soil Sci. Soc. Am. J.*
775 **47**, 873–876.

776 Du Laing G., Rinklebe J., Vandecasteele B., Meers E. and Tack F. M. G. (2009) Trace metal behaviour in
777 estuarine and riverine floodplain soils and sediments: A review. *Sci. Total Environ.* **407**, 3972–3985.

778 Liu R., Ma T., Zhang D., Lin C. and Chen J. (2020) Spatial distribution and factors influencing the
779 different forms of ammonium in sediments and pore water of the aquitard along the Tongshun
780 River, China. *Environ. Pollut.* **266**, 115212.

781 Liu T., Chen D., Luo X., Li X. and Li F. (2019) Microbially mediated nitrate-reducing Fe(II) oxidation:
782 Quantification of chemodenitrification and biological reactions. *Geochim. Cosmochim. Acta* **256**,
783 97–115.

784 Magalhaes C., Costa J., Teixeira C. and Bordalo A. A. (2007) Impact of trace metals on denitrification in
785 estuarine sediments of the Douro River estuary , Portugal. **107**, 332–341.

786 Makowski D. (2019) N₂O increasing faster than expected. *Nat. Clim. Chang.* **9**, 909–910.

787 Marschner B. and Kalbitz K. (2003) Controls of bioavailability and biodegradability of dissolved organic
788 matter in soils. *Geoderma* **113**, 211–235.

789 Martinez-Espinosa C., Sauvage S., Al Bitar A., Green P. A., Vorosmarty C. J. and Sanchez-Perez J. M.
790 (2021) Denitrification in wetlands: A review towards a quantification at global scale. *Sci. Total*
791 *Environ.* **754**.

792 Matocha C. J., Dhakal P. and Pyzola S. M. (2012) The role of abiotic and coupled biotic/abiotic mineral
793 controlled redox processes in nitrate reduction. *Adv. Agron.* **115**, 181–214.

794 Matus F., Stock S., Eschenbach W., Dyckmans J., Merino C., Nájera F., Köster M., Kuzyakov Y. and
795 Dippold M. A. (2019) Ferrous Wheel Hypothesis: Abiotic nitrate incorporation into dissolved
796 organic matter. *Geochim. Cosmochim. Acta* **245**, 514–524.

797 Mehlhorn J., Besold J., Lezama Pacheco J. S., Gustafsson J. P., Kretzschmar R. and Planer-Friedrich B.

798 (2018) Copper mobilization and immobilization along an organic matter and redox gradient -
799 insights from a mofette Site. *Environ. Sci. Technol.* **52**, 13698–13707.

800 Melton E. D., Swanner E. D., Behrens S., Schmidt C. and Kappler A. (2014) The interplay of microbially
801 mediated and abiotic reactions in the biogeochemical Fe cycle. *Nat. Rev. Microbiol.* **12**, 797–808.

802 Merrill L. and Tonjes D. J. (2014) A review of the hyporheic zone, stream restoration, and means to
803 enhance denitrification. *Crit. Rev. Environ. Sci. Technol.* **44**, 2337–2379.

804 Milne C. J., Kinniburgh D. G., Van Riemsdijk W. H. and Tipping E. (2003) Generic NICA - Donnan
805 model parameters for metal-ion binding by humic substances. *Environ. Sci. Technol.* **37**, 958–971.

806 Milne C. J., Kinniburgh D. G. and Tipping E. (2001) Generic NICA-Donnan model parameters for proton
807 binding by humic substances. *Environ. Sci. Technol.* **35**, 2049–2059.

808 Moraghan J. T. and Buresh R. J. (1977) Chemical reduction of nitrite and nitrous oxide by ferrous iron.
809 *Soil Sci. Soc. Am. J.* **41**, 47–50.

810 Mwagona P. C., Yao Y., Yuanqi S. and Yu H. (2019) Laboratory study on nitrate removal and nitrous
811 oxide emission in intact soil columns collected from nitrogenous loaded riparian wetland, Northeast
812 China. *PLoS One* **14**, 1–21.

813 Myneni S. C. B. (2019) Chemistry of natural organic matter—The next step: commentary on a humic
814 substances debate. *J. Environ. Qual.* **48**, 233–235.

815 Nag S. K., Liu R. and Lal R. (2017) Emission of greenhouse gases and soil carbon sequestration in a
816 riparian marsh wetland in central Ohio. **189**, 1–12.

817 Nano G. V. and Strathmann T. J. (2006) Ferrous iron sorption by hydrous metal oxides. *J. Colloid*
818 *Interface Sci.* **297**, 443–454.

819 Nojiri M., Xie Y., Inoue T., Yamamoto T., Matsumura H., Kataoka K., Deligeer, Yamaguchi K., Kai Y.
820 and Suzuki S. (2007) Structure and function of a hexameric copper-containing nitrite reductase.
821 *Proc. Natl. Acad. Sci. U. S. A.* **104**, 4315–4320.

822 Nowicki B. L. (1994) The effect of temperature, oxygen, salinity, and nutrient enrichment on estuarine
823 denitrification rates measured with a modified nitrogen gas flux technique. *Estuar. Coast. Shelf Sci.*
824 **38**, 137–156.

825 Ochoa-Herrera V., León G., Banihani Q., Field J. A. and Sierra-Alvarez R. (2011) Toxicity of copper(II)
826 ions to microorganisms in biological wastewater treatment systems. *Sci. Total Environ.* **412–413**,
827 380–385.

828 Otte J. M., Blackwell N., Ruser R., Kappler A., Kleindienst S. and Schmidt C. (2019) N₂O formation by
829 nitrite-induced (chemo)denitrification in coastal marine sediment. *Sci. Rep.* **9**, 10691.

830 Ottley C. J., Davison W. and Edmunds W. M. (1997) Chemical catalysis of nitrate reduction by iron(II).
831 *Geochim. Cosmochim. Acta* **61**, 1819–1828.

832 Pan Y., Ye L., Ni B. J. and Yuan Z. (2012) Effect of pH on N₂O reduction and accumulation during
833 denitrification by methanol utilizing denitrifiers. *Water Res.* **46**, 4832–4840.

834 Pansu M. and Gautheyrou J. (2006) Handbook of soil analysis: Mineralogical, organic and inorganic
835 methods. In *Springer, Berlin Heidelberg*.

836 Peters B., Casciotti K. L., Samarkin V. A., Madigan M. T., Schutte C. A. and Joye S. B. (2014) Stable
837 isotope analyses of NO₂⁻, NO₃⁻, and N₂O in the hypersaline ponds and soils of the McMurdo Dry
838 Valleys, Antarctica. *Geochim. Cosmochim. Acta* **135**, 87–101.

839 Ponthieu M., Pourret O., Marin B., Schneider A. R., Morvan X., Conreux A. and Cancès B. (2016)
840 Evaluation of the impact of organic matter composition on metal speciation in calcareous soil
841 solution: Comparison of Model VI and NICA-Donnan. *J. Geochemical Explor.* **165**, 1–7.

842 Rahman M. M., Roberts K. L., Grace M. R., Kessler A. J. and Cook P. L. M. (2019) Role of organic
843 carbon, nitrate and ferrous iron on the partitioning between denitrification and DNRA in constructed
844 stormwater urban wetlands. *Sci. Total Environ.* **666**, 608–617.

845 Ren Z. L., Tella M., Bravin M. N., Comans R. N. J., Dai J., Garnier J. M., Sivry Y., Doelsch E., Straathof
846 A. and Benedetti M. F. (2015) Effect of dissolved organic matter composition on metal speciation in
847 soil solutions. *Chem. Geol.* **398**, 61–69.

848 Robertson E. K. and Thamdrup B. (2017) The fate of nitrogen is linked to iron(II) availability in a
849 freshwater lake sediment. *Geochim. Cosmochim. Acta* **205**, 84–99.

850 Robinson T. C., Latta D. E., Notini L., Schilling K. E. and Scherer M. M. (2021) Abiotic reduction of
851 nitrite by Fe(ii): a comparison of rates and N₂O production . *Environ. Sci. Process. Impacts* **23**,
852 1531–1541.

853 Rudnick R. L. and Gao S. (2003) Composition of the continental crust. *The crust* **3**, 1–64.

854 Sakadevan K., Zheng H. and Bavor H. J. (1999) Impact of heavy metals on denitrification in surface
855 wetland sediments receiving wastewater. *Water Sci. Technol.* **40**, 349–355.

856 Sander R. (2015) Compilation of Henry’s law constants (version 4.0) for water as solvent. *Atmos. Chem.*
857 *Phys.* **15**, 4399–4981.

858 Schmidt F., Koch B. P., Goldhammer T., Elvert M., Witt M., Lin Y. S., Wendt J., Zabel M., Heuer V. B.
859 and Hinrichs K. U. (2017) Unraveling signatures of biogeochemical processes and the depositional
860 setting in the molecular composition of pore water DOM across different marine environments.
861 *Geochim. Cosmochim. Acta* **207**, 57–80.

862 Schultz C. and Grundl T. (2004) pH Dependence of ferrous sorption onto two smectite clays.
863 *Chemosphere* **57**, 1301–1306.

864 Seta A. K. and Karathanasis A. D. (1996) Water dispersible colloids and factors influencing their
865 dispersibility from soil aggregates. *Geoderma* **74**, 255–266.

866 Shaaban M., Peng Q. an, Bashir S., Wu Y., Younas A., Xu X., Rashti M. R., Abid M., Zafar-ul-Hye M.,
867 Núñez-Delgado A., Horwath W. R., Jiang Y., Lin S. and Hu R. (2019) Restoring effect of soil
868 acidity and Cu on N₂O emissions from an acidic soil. *J. Environ. Manage.* **250**, 109535.

869 Shampine L. F., Gladwell I. and Thompson S. (2003) *Solving ODEs with MATLAB.*,

870 Shen W., Xue H., Gao N., Shiratori Y., Kamiya T., Fujiwara T., Isobe K. and Senoo K. (2020) Effects of
871 copper on nitrous oxide (N₂O) reduction in denitrifiers and N₂O emissions from agricultural soils.
872 *Biol. Fertil. Soils* **56**, 39–51.

873 Simek M. and Cooper J. E. (2002) The influence of soil pH on denitrification: Progress towards the
874 understanding of this interaction over the last 50 years. *Eur. J. Soil Sci.* **53**, 345–354.

875 Skrabal S. A., Donat J. R. and Burdige D. J. (2000) Pore water distributions of dissolved copper and
876 copper-complexing ligands in estuarine and coastal marine sediments. *Geochim. Cosmochim. Acta*
877 **64**, 1843–1857.

878 Sovacool B. K., Griffiths S., Kim J. and Bazilian M. (2021) Climate change and industrial F-gases: A
879 critical and systematic review of developments, sociotechnical systems and policy options for
880 reducing synthetic greenhouse gas emissions. *Renew. Sustain. Energy Rev.* **141**, 110759.

881 Sparks D. L., Page A. L., Helmke P. A., Loeppert R. H., Soltanpour P. N., Tabatabai M. A., Johnston C.
882 T. and Sumner M. E. (1996) Methods of soil analysis. Part 3: Chemical Methods. In *Soil Science*
883 *Society of America, Madison.*

884 Stumm W. and Sulzberger B. (1992) The cycling of iron in natural environments: Considerations based
885 on laboratory studies of heterogeneous redox processes. *Geochim. Cosmochim. Acta* **56**, 3233–3257.

886 Su J. F., Luo X. X., Wei L., Ma F., Zheng S. C. and Shao S. C. (2016) Performance and microbial
887 communities of Mn(II)-based autotrophic denitrification in a Moving Bed Biofilm Reactor (MBBR).
888 *Bioresour. Technol.* **211**, 743–750.

889 Su J. F., Zheng S. C., Huang T. L., Ma F., Shao S. C., Yang S. F. and Zhang L. N. (2015)
890 Characterization of the anaerobic denitrification bacterium *Acinetobacter* sp. SZ28 and its
891 application for groundwater treatment. *Bioresour. Technol.* **192**, 654–659.

892 Tian H., Chen G., Lu C., Xu X., Ren W., Zhang B., Banger K., Tao B., Pan S., Liu M., Zhang C.,
893 Bruhwiler L. and Wofsy S. (2015) Global methane and nitrous oxide emissions from terrestrial
894 ecosystems due to multiple environmental changes. *Ecosyst. Heal. Sustain.* **1**, 1–20.

895 Tian H., Xu R., Canadell J. G., Thompson R. L., Winiwarter W., Suntharalingam P., Davidson E. A.,
896 Ciais P., Jackson R. B., Janssens-Maenhout G., Prather M. J., Regnier P., Pan N., Pan S., Peters G.
897 P., Shi H., Tubiello F. N., Zaehle S., Zhou F., Arneth A., Battaglia G., Berthet S., Bopp L.,
898 Bouwman A. F., Buitenhuis E. T., Chang J., Chipperfield M. P., Dangal S. R. S., Dlugokencky E.,
899 Elkins J. W., Eyre B. D., Fu B., Hall B., Ito A., Joos F., Krummel P. B., Landolfi A., Laruelle G. G.,

900 Lauerwald R., Li W., Lienert S., Maavara T., MacLeod M., Millet D. B., Olin S., Patra P. K., Prinn
901 R. G., Raymond P. A., Ruiz D. J., van der Werf G. R., Vuichard N., Wang J., Weiss R. F., Wells K.
902 C., Wilson C., Yang J. and Yao Y. (2020) A comprehensive quantification of global nitrous oxide
903 sources and sinks. *Nature* **586**, 248–256.

904 Traina S. J. and Doner H. E. (1985) Heavy metal induced releases of manganese (II) from a hydrous
905 manganese dioxide. *Soil Sci. Soc. Am. J.* **49**, 317–321.

906 Twining B. S., Mylon S. E. and Benoit G. (2007) Potential role of copper availability in nitrous oxide
907 accumulation in a temperate lake. *Limnol. Oceanogr.* **52**, 1354–1366.

908 Wang J., Wang S., Jin X., Zhu S. and Wu F. (2008) Ammonium release characteristics of the sediments
909 from the shallow lakes in the middle and lower reaches of Yangtze River region, China. *Environ.*
910 *Geol.* **55**, 37–45.

911 Wang M., Hu R., Zhao J., Kuzyakov Y. and Liu S. (2016) Iron oxidation affects nitrous oxide emissions
912 via donating electrons to denitrification in paddy soils. *Geoderma* **271**, 173–180.

913 Wang S., Pi Y., Jiang Y., Pan H., Wang Xiaoxia, Wang Xiaomin, Zhou J. and Zhu G. (2020) Nitrate
914 reduction in the reed rhizosphere of a riparian zone: From functional genes to activity and
915 contribution. *Environ. Res.* **180**, 108867.

916 Wang Z., Jiang Y., Awasthi M. K., Wang J., Yang X., Amjad A., Wang Q., Lahori A. H. and Zhang Z.
917 (2018) Nitrate removal by combined heterotrophic and autotrophic denitrification processes: Impact
918 of coexistent ions. *Bioresour. Technol.* **250**, 838–845.

919 Ward B. B., Tuit C. B., Jayakumar A., Rich J. J., Moffett J. and Naqvi S. W. A. (2008) Organic carbon,
920 and not copper, controls denitrification in oxygen minimum zones of the ocean. *Deep. Res. Part I*
921 *Oceanogr. Res. Pap.* **55**, 1672–1683.

922 Waska H., Brumsack H. J., Massmann G., Koschinsky A., Schnetger B., Simon H. and Dittmar T. (2019)
923 Inorganic and organic iron and copper species of the subterranean estuary: Origins and fate.
924 *Geochim. Cosmochim. Acta* **259**, 211–232.

925 Weber K. A., Urrutia M. M., Churchill P. F., Kukkadapu R. K. and Roden E. E. (2006) Anaerobic redox
926 cycling of iron by freshwater sediment microorganisms. *Environ. Microbiol.* **8**, 100–113.

927 Wei J., Ibrahim E., Brüggemann N., Vereecken H. and Mohn J. (2019) First real-time isotopic
928 characterisation of N₂O from chemodenitrification. *Geochim. Cosmochim. Acta* **267**, 17–32.

929 Xu J., Tan W., Xiong J., Wang M., Fang L. and Koopal L. K. (2016) Copper binding to soil fulvic and
930 humic acids: NICA-Donnan modeling and conditional affinity spectra. *J. Colloid Interface Sci.* **473**,
931 141–151.

932 Yan J., Flynn E., Sharma N., Giammar D., Schwartz G., Brooks S., Weisenhorn P., Kemner K.,
933 O’Loughlin E., Kaplan D. and Catalano J. (2021) Consistent Controls on Trace Metal Micronutrient

934 Speciation in Wetland Soils and Stream Sediments. *Geochim. Cosmochim. Acta*.

935 Yan M. and Korshin G. V. (2014) Comparative examination of effects of binding of different metals on
936 chromophores of dissolved organic matter. *Environ. Sci. Technol.* **48**, 3177–3185.

937 Yuan X., Pham A. N., Xing G., Rose A. L. and Waite T. D. (2012) Effects of pH, chloride, and
938 bicarbonate on Cu(I) oxidation kinetics at circumneutral pH. *Environ. Sci. Technol.* **46**, 1527–1535.

939 Zhang C., Yu Z. G., Zeng G. M., Jiang M., Yang Z. Z., Cui F., Zhu M. Y., Shen L. Q. and Hu L. (2014)
940 Effects of sediment geochemical properties on heavy metal bioavailability. *Environ. Int.* **73**, 270–
941 281.

942 Zhao L., Dong H., Edelmann R. E., Zeng Q. and Agrawal A. (2017) Coupling of Fe(II) oxidation in illite
943 with nitrate reduction and its role in clay mineral transformation. *Geochim. Cosmochim. Acta* **200**,
944 353–366.

945 Zhao L., Dong H., Kukkadapu R., Agrawal A., Liu D., Zhang J. and Edelmann R. E. (2013) Biological
946 oxidation of Fe(II) in reduced nontronite coupled with nitrate reduction by *Pseudogulbenkiania* sp.
947 Strain 2002. *Geochim. Cosmochim. Acta* **119**, 231–247.

948 Zhao S., Su X., Wang Y., Yang X., Bi M., He Q. and Chen Y. (2020) Copper oxide nanoparticles
949 inhibited denitrifying enzymes and electron transport system activities to influence soil
950 denitrification and N₂O emission. *Chemosphere* **245**, 125394.

951 Zhu-Barker X., Cavazos A. R., Ostrom N. E., Horwath W. R. and Glass J. B. (2015) The importance of
952 abiotic reactions for nitrous oxide production. *Biogeochemistry* **126**, 251–267.

953 Zhu I. and Getting T. (2012) A review of nitrate reduction using inorganic materials. *Environ. Technol.*
954 *Rev.* **1**, 46–58.

955 Zhu Y. and Elzinga E. J. (2014) Formation of layered Fe(II)-hydroxides during Fe(II) sorption onto clay
956 and metal-oxide substrates. *Environ. Sci. Technol.* **48**, 4937–4945.

957 Zhu Y., Jin X., Tang W., Meng X. and Shan B. (2019) Comprehensive analysis of nitrogen distributions
958 and ammonia nitrogen release fluxes in the sediments of Baiyangdian Lake, China. *J. Environ. Sci.*
959 *(China)* **76**, 319–328.

960

Figures and Tables

Table 1: Cu loadings used for conducting incubation experiments, and dissolved Cu concentrations in the fluid during incubation experiments

Site	Control		Low loading		High loading	
	Cu added ($\mu\text{mol/g}$)	Dissolved conc. (nM)	Cu added ($\mu\text{mol/g}$)	Dissolved conc. (nM)	Cu added ($\mu\text{mol/g}$)	Dissolved conc. (nM)
Riparian 1	N.A	29 \pm 10	0.25	280 \pm 60	1.3	2300 \pm 500
Riparian 2	N.A	41 \pm 9	0.25	97 \pm 10	2.5	560 \pm 40
Stream 1	N.A	3 \pm 1	0.25	16 \pm 2	2.5	53 \pm 7
Stream 2	N.A	6 \pm 2	0.50	52 \pm 6	5.0	590 \pm 30
Marsh 1	N.A	48 \pm 5	0.13	290 \pm 10	0.63	1400 \pm 100

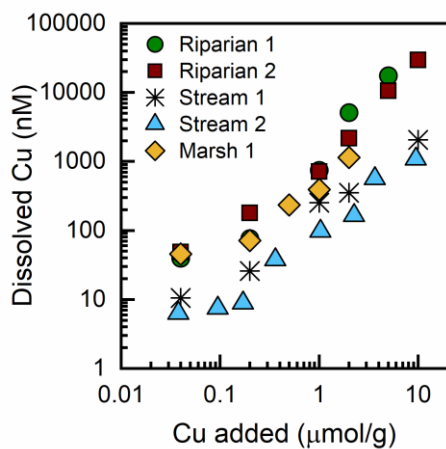


Figure 1: Experimentally determined values of Cu uptake by wetland soils and stream sediments, for use in determining Cu loading in microcosm experiments. Here, Riparian 2 and Riparian 1 represent selected locations from the riparian wetland soil, Marsh 1 from marsh wetland soil, and Stream 2 and Stream 1 are locations from a stream sediment site.

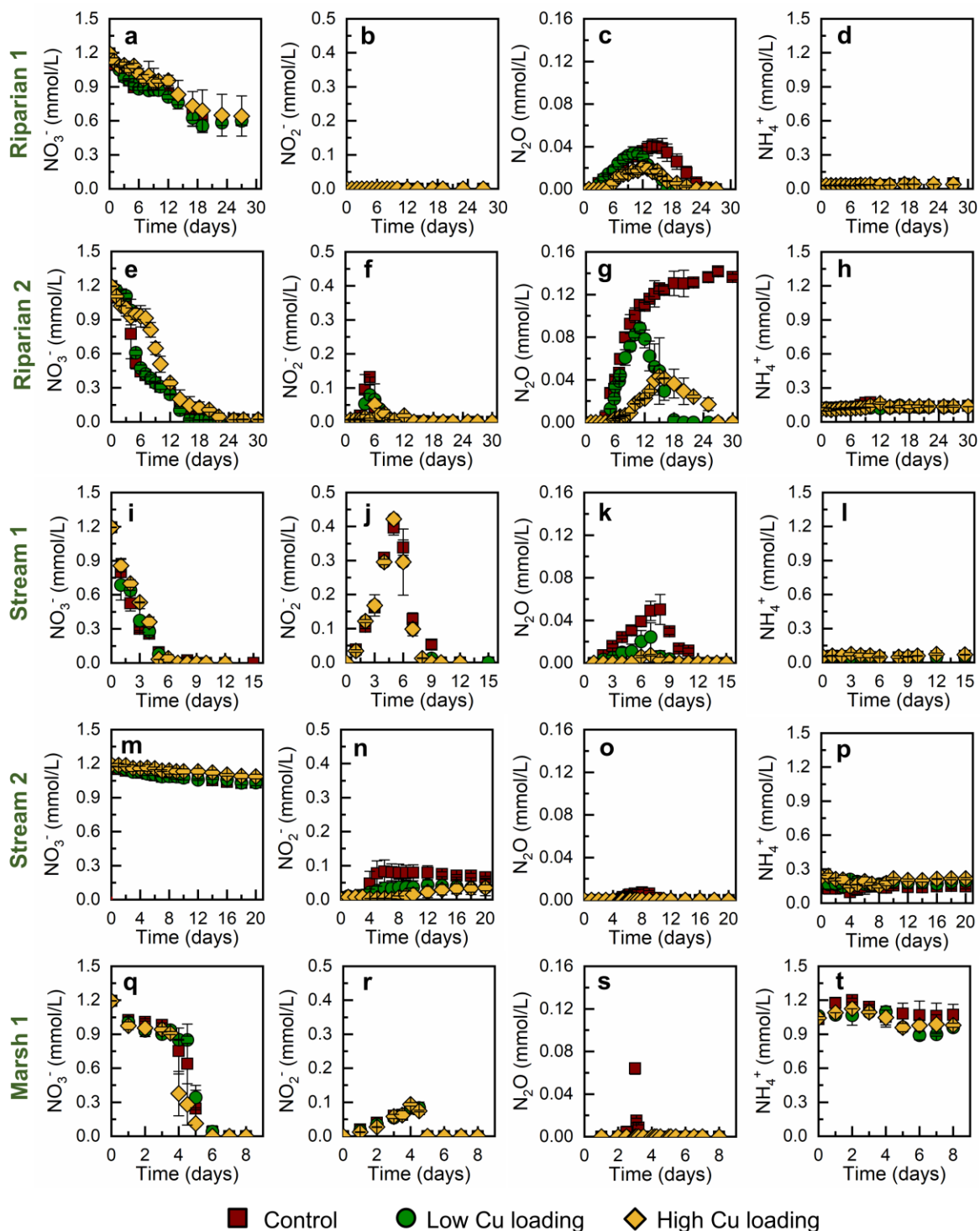


Figure 2: Variation in the concentrations of different N- species (mmol-N L^{-1}) during the incubation experiments for (a-d) Riparian 1, (e-h) Riparian 2, (i-l) Stream 1, (m-p) Stream 2 and (q-t) Marsh 1. In case of low Cu loading, $0.25 \mu\text{mol/g}$ Cu was added in incubation experiments for Riparian 1, Riparian 2, and Stream 1 samples, $0.50 \mu\text{mol/g}$ for Steam 2 and $0.13 \mu\text{mol/g}$ for Marsh 1 incubations. High Cu loading amendments for incubation experiments were $5.0 \mu\text{mol/g}$ for Riparian 1 and Stream 1, $1.3 \mu\text{mol/g}$ for Riparian 2, $5.0 \mu\text{mol/g}$ for Stream 2, and $0.63 \mu\text{mol/g}$ for Marsh 1.

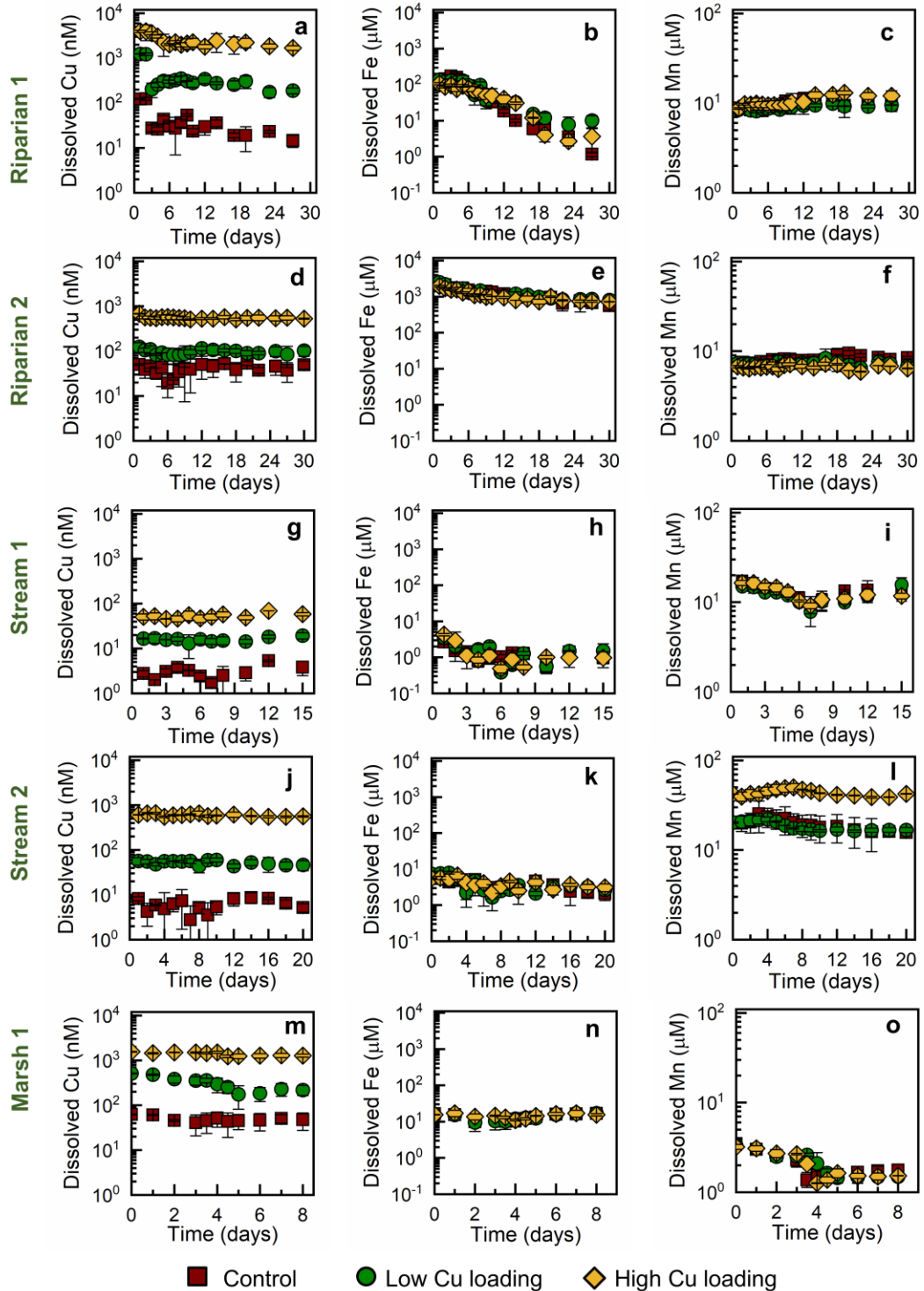


Figure 3: Variation in the concentrations of Cu, Fe and Mn during the incubation experiments for (a-c) Riparian 2, (d-f) Riparian 1, (g-i) Stream 1, (j-l) Stream 2 and (m-o) Marsh 1. In case of low Cu loading, 0.25 $\mu\text{mol/g}$ Cu was added in incubation experiments for Riparian 1, Riparian 2, and Stream 1 samples, 0.50 $\mu\text{mol/g}$ for Stream 2 and 0.13 $\mu\text{mol/g}$ for Marsh 1 incubations. High Cu loading amendments for incubation experiments were 5.0 $\mu\text{mol/g}$ for Riparian 1 and Stream 1, 1.3 $\mu\text{mol/g}$ for Riparian 2, 5.0 $\mu\text{mol/g}$ for Stream 2, and 0.63 $\mu\text{mol/g}$ for Marsh 1.

Table 2: The values of Michaelis-Menten parameters of different reactions involved in carrying out denitrification at different sites as well as the pseudo first-order rate constant for abiotic reduction of NO_2^- to N_2 .

Site	Condition	V_{\max} (mmol L^{-1} day^{-1})	$K_{\text{NO}_3^-}$ (mmol L^{-1})	k_{ab} (day^{-1})	$K_{\text{NO}_2^-}$ (mmol L^{-1})	$K_{\text{N}_2\text{O}}$ (mmol L^{-1})
Riparian 1	Control	0.41±0.02	12±0.5	99±2	0.072±0.004	6900±4
	Low loading	0.41±0.05	11±0.7	99±4	0.072±0.006	24±0.2
	High loading	0.41±0.03	15±0.3	98±5	0.068±0.002	3.5±0.4
Riparian 2	Control	0.25±0.08	1.1±0.1	2.2±0.3	0.68±0.08	11000±8
	Low loading	0.25±0.07	1.1±0.3	2.2±0.9	0.22±0.06	0.48±0.1
	High loading	0.25±0.03	1.7±0.3	2.2±0.4	0.33±0.07	0.21±0.09
Stream 1	Control	0.39±0.06	0.39±0.09	0.69±0.1	9.1±2	3.7±1
	Low loading	0.39±0.07	0.41±0.1	0.71±0.2	9.7±2	0.72±0.4
	High loading	0.39±0.01	0.49±0.01	0.64±0.01	9.5±1	0.00078±0.0003
Stream 2	Control	0.37±0.2	39±3	0.015±0.002	0.079±0.001	0.0085±0.0009
	Low loading	0.37±0.7	40±4	0.015±0.007	0.0067±0.002	0.0024±0.0004
	High loading	0.37±0.02	71±7	0.015±0.001	0.0035±0.001	0.0032±0.0007
Marsh 1	Control	0.27±0.07	0.47±0.2	0.00024±0.0001	0.058±0.008	0.14±0.04
	Low loading	0.27±0.09	0.55±0.2	0.00027±0.0001	0.067±0.002	0.037±0.02
	High loading	0.27±0.04	0.38±0.2	0.00029±0.0001	0.047±0.009	0.018±0.01

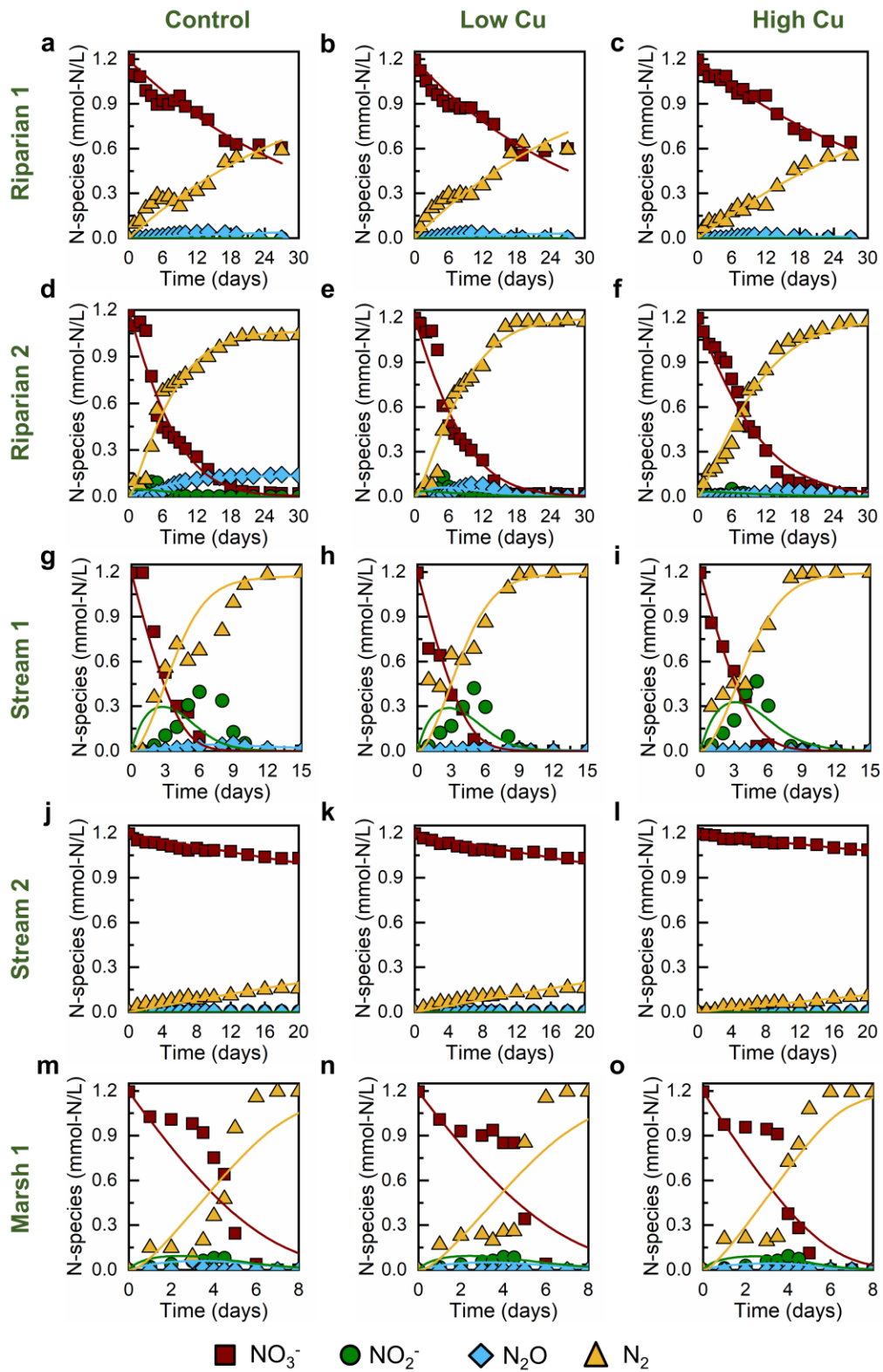


Figure 4: Experimental data together with the output of the optimized kinetic model for the evolution of N-containing species during the incubation experiments using the parameters obtained from the kinetic model for (a-c) Riparian 1, (d-f) Riparian 2, (g-i) Stream 1, (j-l) Stream 2 and (m-o) Marsh 1

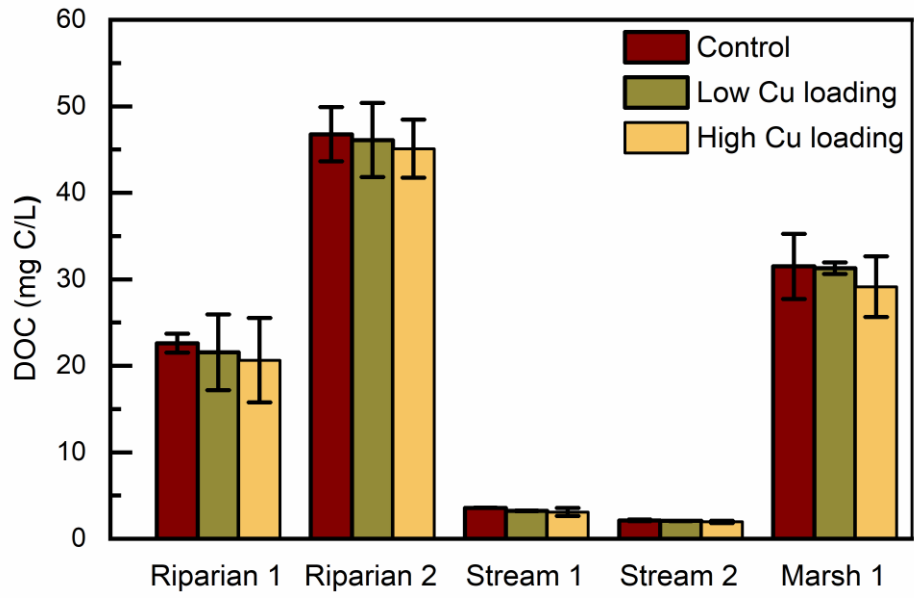


Figure 5: Final dissolved organic carbon concentrations in the incubation experiments with soils and sediments of different natural aquatic systems.

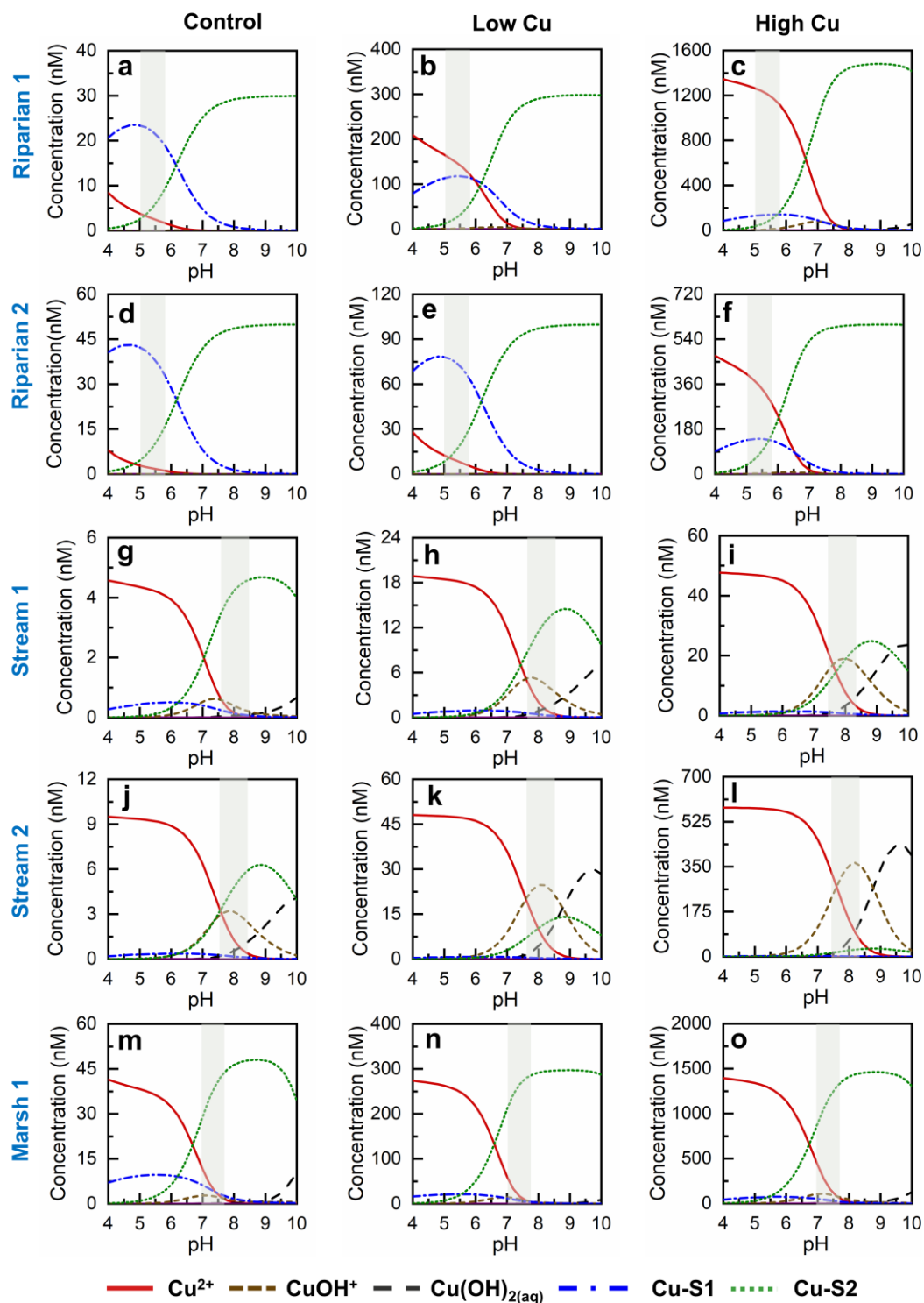


Figure 6: Speciation of dissolved Cu at different concentrations for (a-c) Riparian 2 (d-f) Riparian 1 and (g-i) Stream 2 (j-l) Stream 2 and (m-o) Marsh 1. The concentrations of Cu selected for determining the speciation are based on the dissolved concentration of Cu in the incubation experiments (Table 1). Here, Cu-S1 shows Cu bound to carboxylic acids of organic carbon and Cu-S2 is the Cu bound to phenolic groups on organic carbon. Shaded areas indicate the pH range over the course of the experiment.

SUPPLEMENTARY MATERIAL FOR
Copper availability governs nitrous oxide accumulation in wetland soils and stream sediments

Neha Sharma,¹ Elaine D. Flynn,² Jeffrey G. Catalano² and Daniel E. Giammar¹

¹*Department of Energy, Environmental and Chemical Engineering, Washington University in St. Louis,
St. Louis, Missouri 63130, United States*

²*Department of Earth and Planetary Sciences, Washington University in St. Louis, St. Louis, Missouri
63130, United States*

*Corresponding Author:

Address: Department of Energy, Environmental and Chemical Engineering, Washington University in St. Louis, St. Louis, MO 63130, USA

Phone: (314) 935-6849

Email: giammar@wustl.edu

Geochimica et Cosmochimica Acta

January 2022

This paper is a non-peer reviewed preprint submitted to EarthArXiv

Supplementary material details

Number	Details	Page (s)
Table S1	Concentration of major elements and species in the simulated site water used for uptake studies and microcosm experiments	3
Table S2	Characterization of soils and sediments collected from different aquatic systems	3
Section S1	Dissolved Cu speciation in microcosms	4
Table S3	Parameters used in NICA-Donnan model for determining Cu speciation in the presence of DOC	5
Table S4	Estimated labile concentrations of Cu in the microcosms using NICA-Donnan model	5
Section S2	Estimation of organic carbon requirements for complete reduction of nitrate	6
Section S3	Estimation of nitrate requirements for abiotic reaction with Fe(II)	7
Figure S1	Variation in the concentration of NO_3^- during incubation period at different sites studied. The scale on the plots is selected to show changes in NO_3^- for the earliest reaction times.	8

1 Table S1: Concentration of major elements and species in the simulated site water used for uptake studies
 2 and microcosm experiments

Parameter	ANL	ORNL	TB	3
pH	7.0	7.6	5.0	
Ionic Strength	1.7 mM	7.0 mM	0.30 mM	
Concentration (μM)				
Na ⁺	170	450	60	
K ⁺	170	71	5.3	
Ca ²⁺	370	1100	25	
Mg ²⁺	290	390	27	
Cl ⁻	490	2700	160	
SO ₄ ²⁻	580	260	7.6	
NO ₃ ⁻	8	70	0	
NH ₄ ⁺	0	0.2	0	
PO ₄ ³⁻	0	4	0	

4
 5 Table S2: Characterization of soils and sediments collected from different aquatic systems (Yan et al.)

Site	Cu (nmol/g)	Mn (nmol/g)	Fe ($\mu\text{mol/g}$)	C (%)	S (%)	NH ₄ ⁺ ($\mu\text{mol/g}$)	NO ₂ ⁻ ($\mu\text{mol/g}$)	NO ₃ ⁻ ($\mu\text{mol/g}$)
Riparian 1	48	220	47	1.3	0.02	1.1	BDL	0.14
Riparian 2	260	701	460	6.0	0.09	2.7	BDL	0.00
Stream 1	160	3200	204	3.0	0.10	2.7	BDL	0.14
Stream 2	98	5600	420	0.46	0.02	2.8	BDL	0.43
Marsh 1	280	1960	420	9.0	0.24	21	BDL	0.36

6 Here, nutrients represent the extractable values from soils and sediments. Total Cu, Mn, and Fe concentrations
 7 present in soils and sediments were obtained using microwave-assisted digestion technique. Carbon and sulfur
 8 percent were estimated using CHNS analyzer. The detection limit of NO₂⁻ is 0.02 $\mu\text{mol/g}$.

9 Section S1: Dissolved Cu speciation in microcosms

10 Two different binding sites are considered in the NICA model, type 1 and type 2, corresponding
 11 to carboxylic (low affinity) and phenolic (high affinity) sites respectively (Benedetti et al., 1995).

$$12 \quad Q_i = \frac{n_{i,1}}{n_{H,1}} Q_{\max 1,H} \frac{(\hat{K}_{i,1} c_i)^{n_{i,1}} [\sum (\hat{K}_{i,1} c_i)^{n_{i,1}}]^{p_1}}{\sum (\hat{K}_{i,1} c_i)^{n_{i,1}} + [\sum (\hat{K}_{i,1} c_i)^{n_{i,1}}]^{p_1}} + \frac{n_{i,2}}{n_{H,2}} Q_{\max 1,H} \frac{(\hat{K}_{i,2} c_i)^{n_{i,2}} [\sum (\hat{K}_{i,2} c_i)^{n_{i,2}}]^{p_2}}{\sum (\hat{K}_{i,2} c_i)^{n_{i,2}} + [\sum (\hat{K}_{i,2} c_i)^{n_{i,2}}]^{p_2}}$$

13 Eq S1

14 where, c_i (mol. L⁻¹) is the concentration of metal; Q_i is the amount of bound ion described by two identical
 15 binding expressions, one each for the carboxylic- (1) and phenolic-type (2) site
 16 distributions. $Q_{\max 1,H}$ and $Q_{\max 2,H}$ are the maximum proton binding capacity of humic substances within
 17 each distribution (mol kg⁻¹); p_1 and p_2 account for intrinsic heterogeneity of humic substances; $\hat{K}_{i,1}$ and
 18 $\hat{K}_{i,2}$ are median values for affinity distributions for ion, and $n_{i,1}$ and $n_{i,2}$ are used to describe the nonidealities
 19 of the ion-binding to each distribution. The ratios $\frac{n_{i,j}}{n_{H,j}}$ with $j = 1$ or 2 reflect the average stoichiometry of ion
 20 binding.

21 The charge on humic substances is neutralized by the nonspecific binding of counter-ions and
 22 exclusion of co-ions within the Donnan volume, V_D (L·kg⁻¹), as described by the empirical relationship.

$$23 \quad \log V_D = b(1 - \log I) - 1 \quad \text{Eq S2}$$

24 Here, I is ionic strength and b is an empirical parameter describing the variation of Donnan volume with
 25 ionic strength (Benedetti et al., 1996). The values of parameters used in estimating Cu speciation are listed
 26 in Table S3.

27 Humic substances are normally assumed to be the main binding substances (Ren et al., 2015), and
 28 their concentrations were determined from the dissolved organic carbon (DOC) concentrations. Humic
 29 substances account for 60% of DOC in natural water systems (Zhang and Davison, 2000; Gueguen et al.,
 30 2011), and they comprise 50% carbon, so concentration of HS was assumed to be 1.2 times the DOC
 31 concentration. The pH, temperature, total dissolved elements (Na, Mg, K, Ca, Cl, NO₃, SO₄, and PO₄)
 32 (Table EA1), and dissolved Cu, Fe, and Mn were used as the input parameters for determining Cu speciation.

33 Table S3: Parameters used in NICA-Donnan model for determining Cu speciation in the presence of DOC
 34 (Xu et al., 2016)
 35

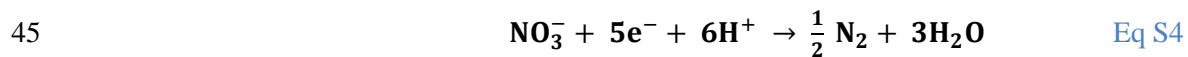
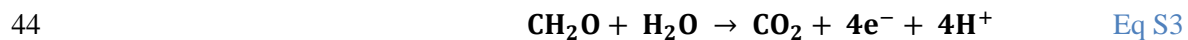
Parameter	Value
<i>b</i>	0.57
$Q_{\max 1,H}$	5.88
p_1	0.59
$\log k_{H,1}$	2.34
$n_{H,1}$	0.66
$\log k_{Cu,1}$	0.26
$n_{Cu,1}$	0.53
$Q_{\max 2,H}$	1.86
p_2	0.70
$\log k_{H,2}$	8.60
$n_{H,2}$	0.76
$\log k_{Cu,2}$	8.26
$n_{Cu,2}$	0.36

36
 37
 38 Table S4: Estimated labile concentrations of Cu in the microcosms using NICA-Donnan model
 39

Site	Estimated labile concentration (nM)*		
	Control	Low Cu	High Cu
Riparian 1	2.8 ± 0.9	150 ± 20	1200 ± 80
Riparian 2	1.4 ± 0.8	8.9 ± 3	350 ± 60
Stream 1	0.55 ± 0.3	7.2 ± 2	28 ± 4
Stream 2	4.8 ± 0.9	38 ± 3	560 ± 4
Marsh 1	7.6 ± 5	35 ± 30	150 ± 100

40 *Labile Cu concentration is the sum of Cu, CuOH⁺, and Cu(OH)₂. The values represent the average of the labile
 41 concentrations between the pH range studied. pH varied between 5-6 in wetland soils; 7.6-8.6 in stream sediments,
 42 and 7-8 in marsh wetland soils.

43 Section S2: Estimation of organic carbon requirements for complete reduction of nitrate



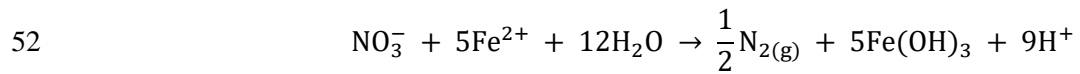
47 Total nitrate available=0.05 mmol

48 Total organic carbon (OC) requirement = 0.0625 mmol

Site	Organic Carbon (%)	Total organic carbon (mmol)	$\frac{TOC}{OC_{required}}$
Riparian 2	6.0	13	208
Riparian 1	1.3	2.7	43
Stream 1	3.1	6.3	101
Stream 2	0.46	0.77	12
Marsh 1	9.0	19	304

49 *Here, total organic carbon represents the total amount of organic carbon present in the solid phase (2.5 g of
50 soil/sediment) used for incubation experiments.

51 Section S3: Estimation of nitrate requirements for abiotic reaction with Fe(II)



53 **Riparian 1:**

54 Decrease in Fe : 7.1 μmol

55 NO_3^- required: 1.4 μmol

56 **Riparian 2:**

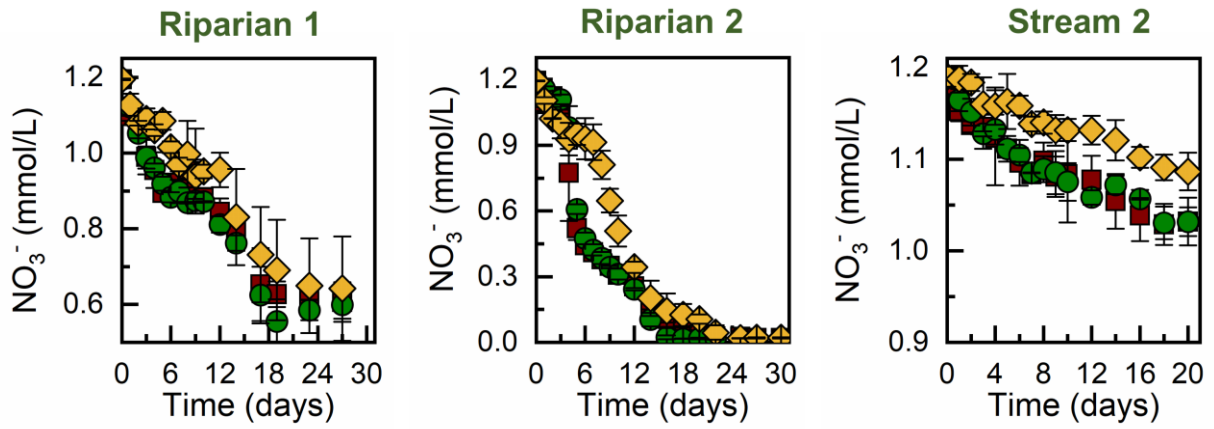
57 Decrease in Fe concentration: 72 μmol

58 NO_3^- required: 14 μmol

59 **Stream 1:**

60 Decrease in Fe concentration: 0.084 μmol

61 NO_3^- required: 0.017 μmol



62

63

64

Figure S1: Variation in the concentration of NO_3^- during incubation period at different sites studied. The scale on the plots is selected to show changes in NO_3^- for the earliest reaction times.

65 **References**

- 66 Benedetti M. F., Milne C. J., Kinniburgh D. G., Van Riemsdijk W. H. and Koopal L. K. (1995) Metal ion
67 binding to humic substances: Application of the non-ideal competitive adsorption model. *Environ.*
68 *Sci. Technol.* **29**, 446–457.
- 69 Benedetti M. F., Van Riemsdijk W. H. and Koopal L. K. (1996) Humic substances considered as a
70 heterogeneous Donnan gel phase. *Environ. Sci. Technol.* **30**, 1805–1813.
- 71 Gueguen C., Clarisse O., Perroud A. and McDonald A. (2011) Chemical speciation and partitioning of
72 trace metals (Cd, Co, Cu, Ni, Pb) in the lower Athabasca river and its tributaries (Alberta, Canada).
73 *J. Environ. Monit.* **13**, 2865–2872.
- 74 Ren Z. L., Tella M., Bravin M. N., Comans R. N. J., Dai J., Garnier J. M., Sivry Y., Doelsch E., Straathof
75 A. and Benedetti M. F. (2015) Effect of dissolved organic matter composition on metal speciation in
76 soil solutions. *Chem. Geol.* **398**, 61–69.
- 77 Xu J., Tan W., Xiong J., Wang M., Fang L. and Koopal L. K. (2016) Copper binding to soil fulvic and
78 humic acids: NICA-Donnan modeling and conditional affinity spectra. *J. Colloid Interface Sci.* **473**,
79 141–151.
- 80 Zhang H. and Davison W. (2000) Direct in situ measurements of labile inorganic and organically bound
81 metal species in synthetic solutions and natural waters using diffusive gradients in thin films. *Anal.*
82 *Chem.* **72**, 4447–4457.
- 83